Scaling Laws for Robust Comparison of Open Foundation Language-Vision Models and Datasets

Marianna Nezhurina[1,2,5§*] **Tomer Porian**[1,2,5*] **Giovanni Puccetti**[3] **Tommie Kerssies**[1,4]
Romain Beaumont[1] **Mehdi Cherti**[1,2,5§°*] **Jenia Jitsev**[1,2,5°*]
[1]LAION [2]Juelich Supercomputing Center (JSC), Research Center Juelich (FZJ)
[3] Institute of Information Science and Technologies "A. Faedo" - CNR Pisa
[4] Eindhoven University of Technology
[5] Open-Ψ (Open-Sci) Collective
§ equal first, ° equal senior, * core contribution
{m.nezhurina,m.cherti,j.jitsev}@fz-juelich.de,contact@laion.ai

Abstract

In studies of transferable learning, scaling laws are obtained for various important foundation models to predict their properties and performance at larger scales. Taking language-vision learning as example, we show here how scaling law derivation can also be used for model and dataset comparison, allowing to decide which procedure is to be preferred for pre-training. Full scaling laws based on dense measurements across a wide span of model and samples seen scales are derived for two important language-vision learning procedures, CLIP and MaMMUT, that use either contrastive only or contrastive and captioning text generative loss. For the first time, we use derived scaling laws to compare both models and three open datasets, DataComp-1.4B, Re-LAION-1.4B and DFN-1.4B, while ensuring sufficient prediction accuracy on held out points. From comparison, we obtain evidence for (i) MaMMUT's stronger improvement with scale and better sample efficiency than standard CLIP (ii) DFN-1.4B outperforming other open datasets. To strengthen validity of the comparison, we show scaling laws for various downstream tasks, classification, retrieval, and segmentation, observing consistently the same scaling trends for models and datasets across tasks. We show that comparison can also be performed when deriving scaling laws with a constant learning rate schedule, reducing compute cost. Accurate derivation of scaling laws provides thus means to perform model and dataset comparison on aligned common compute axis across large scale span, avoiding misleading conclusions based on measurements from few isolated single reference scales only. This paves road for guided collective improvement of open foundation models and training datasets, as scaling law based comparisons from various studies executed in common frame can be combined to identify overall better procedures. We release all the pre-trained models with their intermediate checkpoints, including openMaMMUT-L/14, which achieves 80.3% zero-shot ImageNet-1k accuracy, trained on 12.8B samples from DataComp-1.4B[1].

1 Introduction

Foundation models [1] pre-trained on generic, diverse large datasets enabled massive improvements in transfer learning, showing strong and efficient adaptability across a wide range of downstream tasks not shown during pre-training. Thanks to learning procedures leading to foundation models,

[1] Code for reproducing experiments in the paper and raw experiments data can be found in the repository

39th Conference on Neural Information Processing Systems (NeurIPS 2025).

transferable learning can be studied across various important domains, including language [2, 3, 4], vision [5], language-audio [6], and language-vision [7].

Progress in improving learning procedures leading to stronger foundation models crucially depends on the ability to perform systematic and consistent learning procedure comparison. Usually, following the training, various foundation models are compared via performance shown on a wide range of standardized reference downstream tasks. Often, this comparison is done on only one or few selected reference model and data scales, without carefully aligning the compute put into pre-training. Further, important parts of learning procedure like training dataset often remain closed. This makes it hard or impossible to discern whether the observed model differences are due to algorithmic, dataset or due to differences in pre-training compute, or a combination of them, leaving also unclear whether the comparison holds for other scales than the few selected ones.

In our work, we make a step towards resolving these issues by using scaling law derivation to enable systematic training procedure, model, and dataset comparison. Foundation models exhibit scaling laws [8, 9, 10, 11] that allow to determine dependence of model properties and performance on total pre-training compute from measurements on smaller scales, enabling predictions across a wide scale span instead of only one or few selected points. Here, we show how using open datasets for scaling law derivation can enable model and dataset comparison that takes into account model behavior across a wide range of pre-training compute budgets and across different downstream tasks, while offering full control over variations in the whole training pipeline, and being fully reproducible.

We choose language-vision learning as an important setting for model and dataset comparison using scaling law derivation. Contrastive language-image pre-training (CLIP) [7] is a well-established learning procedure resulting in models that show impressive robustness and transfer capability, and are used routinely as pre-trained components in many setups such as vision-language instruction tuning models (LLaVa [12], InternVL [13], SigLIP [14]) and text to image generation models [15]. Since the first release of CLIP, many extensions have been proposed such as CoCa [16], MaMMUT [17], and SigLIP [18, 14]. These works claim more performant language-vision models than standard CLIP. However, as hinted above, it is still unclear which of the training procedures are better for what reasons, and whether claims of improving on the standard CLIP procedure hold across scales. Here, we conduct a large-scale study of the scaling laws of two important procedures, namely CLIP and MaMMUT, pre-trained on open reference datasets, DataComp-1.4B [19], DFN-1.4B [20] and Re-LAION-1.4B [21], which we are able to compare via full scaling law derivation for the first time.

Our study reveals that while CLIP has advantage on smaller compute scales, MaMMUT architecture shows advantage as we increase compute, as illustrated by cross-over of the scaling curves in Fig. 1, 2,3 (Sec. 3.1). Importantly, we find that the comparison via scaling laws delivers result that is consistent and robust across the pre-training datasets, learning schedules and the downstream tasks.

Our Contributions. 1) We conduct first large-scale study of CLIP [7, 10] and MaMMUT [17] with dense measurements to ensure better prediction to unseen scales and valid model and dataset comparison. Measurements cover model sizes from S/32 to H/14, samples seen from 1.28M to 3B, training on DataComp-1.4B [19], Re-LAION-1.4B [21] and DFN-1.4B [20] datasets and evaluating downstream performance on tasks covering zero-shot classification, retrieval, and segmentation. **2)** Based on derived scaling laws, we perform model and dataset comparison. We show validity of this comparison by revealing consistent trends in favor of MaMMUT versus CLIP architecture across different downstream tasks and pretraining datasets, as well as distinct scaling law types (compute-optimal and samples seen based scaling laws). We also show consistent trends favoring DFN-1.4B over other datasets. Our study is thus the first to provide a fully reproducible systematic comparison of important open foundation models openCLIP and openMaMMUT and important reference open datasets Re-LAION-1.4B, DataComp-1.4B and DFN-1.4B. **3)** We perform the study using both cosine and constant learning rate schedules, and observe the same consistent trends, revealing that the scaling laws based comparison can be also performed with suboptimal constant learning rate schedule resulting in 98% less compute cost. **4)**. We provide a detailed procedure to fit scaling laws tailored for model and dataset comparison, sharing our findings on best practices of scaling law derivation which include uncertainty quantification and measuring held-out points on the compute or samples-seen axis. **5)** We make our study fully reproducible and release all the intermediate checkpoints from scaling law derivation experiments. For the first time, we provide an open-source implementation of MaMMUT, openMaMMUT, and release openMaMMUT-L/14 trained on 12.8B image-text samples from an open dataset DataComp-1.4B, achieving 80.3% zero-shot ImageNet-1k accuracy.

2 Methods & experimental setup

Our experiments entail model pre-training, evaluation and scaling law derivation, which we describe in the following.

2.1 Pre-training setup

Architecture details. The MaMMUT model is integrated into the `openCLIP` code base [22] to take advantage of the existing implementation of the CLIP contrastive loss and CoCa captioning loss. Key additions to implement MaMMUT were: (1) using a double forward pass for the text component to perform both text encoding (without masking) and decoding (with causal masking); (2) cross-attention between image and text tokens. For an N-layer text decoder, cross-attention layers are inserted every 2 text decoder layers [17], a total of $[\frac{N}{2}]$ cross-attention layers.

Training dataset & objective. We pre-trained CLIP and MaMMUT models on DataComp-1.4B [19], Re-LAION-1.4B [21] and DFN-1.4B [20] datasets. Re-LAION-1.4B was obtained by downloading the `Re-LAION-2B-en-research` subset of Re-LAION [21] which contained $\approx$ 30% dead links, resulting in a total of 1.4B image-caption pairs. DFN-1.4B was obtained by downloading DFN-2B dataset [20], which also resulted in discovering $\approx$ 30% link rot, again providing 1.4B image-text pairs in total. CLIP models are trained with contrastive InfoNCE [23] loss ($L = L_{\text{contrastive}}$), while MaMMUT models are trained with contrastive and captioning losses ($L = L_{\text{contrastive}} + \lambda L_{\text{cap}}$), we used $\lambda = 1$ in our experiments.

Model & samples seen scales. For both CLIP and MaMMUT architectures, we consider ViT-S, ViT-M, ViT-B, ViT-L, and ViT-H as vision encoders. For each vision encoder size, we also vary patch size, and consider patch sizes of 32x32, 16x16, and 14x14, leading to $|M| = 15$ model configurations. We scale text encoders accordingly following previous literature [10]. For samples seen scales D, we consider a wide range of measurements $D = \{1.28\text{M}, 3.07\text{M}, 6.4\text{M}, 12.8\text{M}, 30.7\text{M}, 64\text{M}, 128\text{M}, 307\text{M}, 640\text{M}, 1.28\text{B}, 3.07\text{B}\}$, a total of $|D| = 11$ configurations. See App. Tab. 14 for full details about models and number of samples we used in our experiments. To rule out effects of training trial-to-trial variance on measurements and scaling law derivation, we estimate variance of downstream performance across training repetitions in the control experiment (App. Tab. 7).

Learning rate schedule. In our experiments, we consider both cosine and constant learning rate schedulers. For cosine learning rate schedule experiments, we performed a single run for each model-samples seen pair, while for constant learning rate schedule, we only need to train once for each model size.

Optimization. We perform a hyper-parameter sweep for batch size, learning rate and warmup for each training run to avoid suboptimal solutions. We have observed that it is important, especially in small sample seen scales, as large batch sizes usually used in CLIP training will result in small number of optimization steps, making optimization suboptimal. For training, we used AdamW [24] as an optimizer with a weight decay of 0.2. To avoid unstable training and loss spikes with larger models (e.g., ViT-L, ViT-H) we followed [10, 25] and used $\beta_1 = 0.9$, $\beta_2 = 0.95$, gradient clip norm of 1, warmup and mixed precision with `bfloat16`. See more details in App. Tab. 13 and 12.

2.2 Downstream evaluation

Zero-shot classification. We evaluate the top-1 zero-shot accuracy on 35 classification tasks from the DataComp evaluation suite [19]. It includes ImageNet-1k [26], ImageNet robustness to distribution shift datasets [27, 28, 29, 30, 31], and additional 29 classification tasks covering multiple domains. We follow the evaluation protocol of [10], i.e. using the same prompts, class names, and code base [32]. The full list of datasets we used in evaluation with description is included in Appendix F.

Zero-shot retrieval. We evaluate models on MS-COCO[33] image and text retrieval Recall@5 metrics, following [10].

Segmentation. We fine-tune for semantic segmentation on ADE20K [34], following [35], using 31 epochs and a 1500-step warmup [36], with a consistent 224×224 input and 14×14 patch size.

2.3 Scaling law derivation and fitting procedure

We vary both model architecture size (number of parameters of both text and vision towers), number of samples seen and patch size. In general, the relationship between compute and performance follows a power law: $\mathcal{L} = aC^b$, where C is compute in FLOPs [10, 37], with the set of points $\{C, \mathcal{L}(C)\}$ located on the Pareto frontier. Since we use error rate on ImageNet-1k zero-shot classification, we follow [37, 38] and take into account the saturation (B_c) that occurs at the small compute scales due to the nature of classification tasks - the probability of predicting a class even at zero-compute is determined by the frequency of this class in the test set. On the other hand, tasks like zero-shot image classification cannot be solved with 100% accuracy due to task- and learning method-intrinsic performance ceiling [38, 37]. Accordingly, we require that our scaling law functional form satisfies:

$$\mathcal{L}(C) > 0 \text{ (strictly positive)}, \quad \lim_{C\to\infty} \mathcal{L}(C) = E \text{ (irreducible error)}, \quad \frac{d\mathcal{L}}{dC} < 0 \text{ (monotonic decrease).}$$

Given above criteria, we obtain the following functional form for the error that satisfies all three (subscript C specifies compute dependency):

$$\mathcal{L}(C) = A_c \cdot (C + B_c)^{-\alpha_c} + E_c,\ \alpha_c > 0 \tag{1}$$

For each combination of compute scale C and model architecture, we take a point with the minimal error rate. In previous works [39], points with minimal loss were found by binning FLOP values into 1500 FLOP logarithmically spaced intervals. We use the same approach to find points with minimal error. Therefore, we obtain a mapping from each combination of number of parameters N and samples seen D to the compute C (in GFLOPs). Using measurements $\{(C_i, Y_i)\}$ where C_i is compute budget (GFLOPs) and Y_i is error performance, we fit the curve only on points with compute budget below a threshold $\{(C_i, Y_i), C_i < C_{\text{threshold}}\}$. To quantify the quality of our fit, we use mean squared error on the remaining (held-out) points: $\text{MSE} = \frac{1}{n}\sum_{i:C_i \geq C_{\text{threshold}}}(\mathcal{L}(C_i) - Y_i)^2$.

2.4 Confidence intervals estimation

We estimate 95% confidence intervals for the model parameters by propagating the uncertainty from the estimated parameters. We compute the Jacobian of the model, J, with respect to the parameters at the extrapolated points. We then estimate the variance of our predictions as $\sigma^2 = J^\top \,\text{Cov}(\hat{\theta})\, J$. Confidence intervals are then given by $\hat{y} \pm t_{\alpha/2,\, n-p} \cdot \sigma$, where $t_{\alpha/2,\, n-p}$ is the critical value from the Student's t-distribution at $\alpha = 0.05$.

2.5 Data efficiency and optimal dataset size estimation

To quantify the data efficiency of CLIP and MaMMUT, we fit a scaling law analogous to Equation 1:

$$\mathcal{L}(D) = A_D \cdot (D + B_D)^{-\alpha_D} + E_D \tag{2}$$

Here, $\mathcal{L}(D)$ denotes the expected error rate as a function of the number of samples seen D. For each unique data budget D, we extract the corresponding minimal error points $\{D, \mathcal{L}(D)\}$ using the Skyline Operator algorithm [40], which selects non-dominated configurations based on error rate.

To estimate the dataset size that is optimal for a given compute budget, we follow the approach of [9] and fit a power-law relationship of the form: $D_{\text{opt}} = D_0 \cdot C^a$, where D_{opt} minimizes $\mathcal{L}(C, D)$ for a given compute budget C. The optimal dataset sizes are obtained by identifying (C, D) pairs that yield minimal error rate under fixed compute constraints.

3 Results

3.1 Scaling laws for model and dataset comparison

We fit function that has a form of Eq. 1 on the obtained experimental data using methods described in Section 2.3. To avoid the confound of data repetition [41] we limit the data used for our scaling law fits by selecting only models that were trained on up to 3B. In Tab. 5a estimated parameters for both models (CLIP and MaMMUT) as well as for both downstream tasks (IN1k classification

Model Candidate	Samples Seen Candidate	GFLOPs	IN1k acc1 Predicted (95% CI)
ViT-L-14	12.8B	2.14e+12	0.796 (0.788, 0.804)
ViT-L-14	15.5B	2.59e+12	0.800 (0.791, 0.808)
mammut-ViT-L-14	10.6B	2.14e+12	0.816 (0.811, 0.821)
mammut-ViT-L-14	12.8B	2.59e+12	0.820 (0.815, 0.826)

Table 1: Estimation of IN1k performance for CLIP and MaMMUT on unseen compute scales using our scaling laws fits. Additionally, for each compute scale, we provide possible models and samples seen (assuming unique samples) sizes.

and MS-COCO retrieval) can be found. **MaMMUT consistently exhibits better scaling behaviour** compared to CLIP. This is reflected in smaller error rates at equivalent compute budget at larger scales after crossing a compute threshold that is consistently found to be between 10^{10} and 10^{11} GFLOPS across various datasets and tasks (Fig. 1, 2,3). Note that on smaller scales in the lower performance range, CLIP consistently outperforms MaMMUT, which then consistently takes over CLIP at larger compute scales in the higher performance range. This indicates better efficiency and generalization as we increase compute. This trend holds across:

- Pre-training datasets: DataComp-1.4B (Fig. 1), Re-LAION-1.4B (Fig. 2) and DFN-1.4B (Fig. 3).
- Downstream tasks: ImageNet-1k zero-shot image classification (see Fig. 1 (a), Fig. 2 (a)) and MS-COCO image retrieval (Fig. 1 (b), Fig. 2 (b)), ADE20K semantic segmentation (Fig. 6).
- Learning rate scheduler: cosine (Fig. 1) and constant (Fig. 5).

We validate our fits by fitting the laws only up to certain compute budgets $C_{\text{threshold}}$ and then extrapolating to larger ones. We use these extrapolated points to compute MSE, which allows us to check on quality of the obtained fits, observing that adding more points to the fit reduces MSE on held-out points and also reduces uncertainty of predictions. The measured performance falls well within the prediction confidence interval (App. Tab. 10). Detailed versions of scaling laws plots for CLIP and MaMMUT can be found in Appendix B, more details on validating fit quality are in Appendix C. As further evidence for the validity of derived scaling laws, we observe same consistent scalability trends across datasets and on further important downstream tasks, for instance on DataComp eval suite (Fig. 14), ImageNet robustness (Fig. 15), or on segmentation after fine-tuning (Fig. 6), see Sec. F.

In Tab. 1 we provide predictions on DataComp-1.4B for both MaMMUT and CLIP for unseen compute budgets 2.14e+12 GFLOPs (corresponds to CLIP ViT-L-14 trained on 12.8B image-text pairs) and 2.59e+12 GFLOPs (corresponds to MaMMUT ViT-L-14 trained on 12.8B samples). We see that our predictions favor MaMMUT over CLIP. As a prediction test on larger scales further away, for CLIP ViT-L-14 trained on 12.8B samples of DataComp-1.4B our prediction for ImageNet-1k 0-shot accuracy (79.6%) is close to performance of CLIP ViT-L-14 trained on 12.8B samples reported in the original DataComp work [19] - 79.2%. Note that the measured performance IN1K zero-shot 79.2% in the DataComp original work [19] was done with heavy samples repetitions (12.8B on DataComp-1.4B is about 9x), while our prediction is done for unique or low repetition scenario, which also might explain tendency to a higher performance in the predictions than observed in experiments on 12.8B samples seen scale (Tab. 1).

As evident from Fig. 9 and 10, **DFN-1.4B consistently provides stronger scalability** compared to DataComp and Re-LAION, for both CLIP and MaMMUT architectures and for both zero-shot ImageNet-1k classification and MS-COCO retrieval. Despite lower compute used for dataset comparison and higher uncertainty for the trends resulting from fewer measurements for DFN, measured trends are clear and consistent, allowing thus to draw conclusions favoring DFN-1.4B over other datasets in the comparison.

3.2 Data efficiency and compute-optimal dataset size

Fig. 4 illustrates that MaMMUT exhibits **superior data efficiency** relative to CLIP. In Fig. 4 (a) we see that MaMMUT achieves better performance on ImageNet-1k zero-shot image classification as the number of training samples increases. In Fig. 4 (b) MaMMUT requires fewer training samples to achieve compute optimal performance on ImageNet-1k zero-shot classification. This indicates that

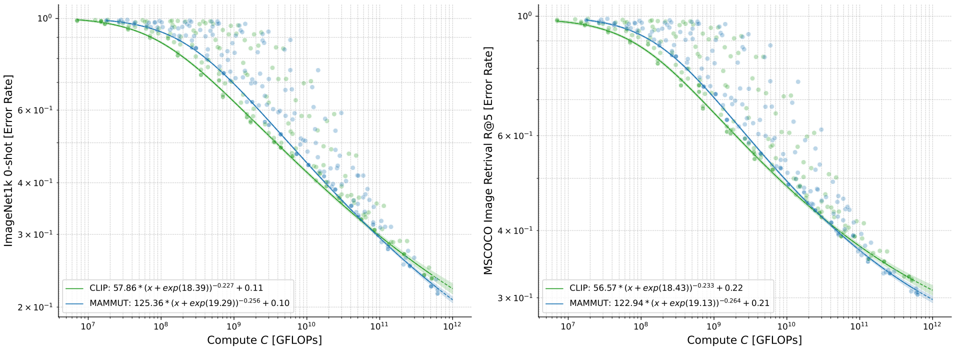

(a) ImageNet-1k 0-shot classification

(b) MS-COCO image R@5

Figure 1: **Scaling on DataComp-1.4B.** Comparison of CLIP and MaMMUT via scaling laws on DataComp-1.4B. Error rate on downstream tasks is plotted against compute. MaMMUT outperforms CLIP in terms of scalability, with scaling law fit lines crossing close to 10^{11} GFLOPS.

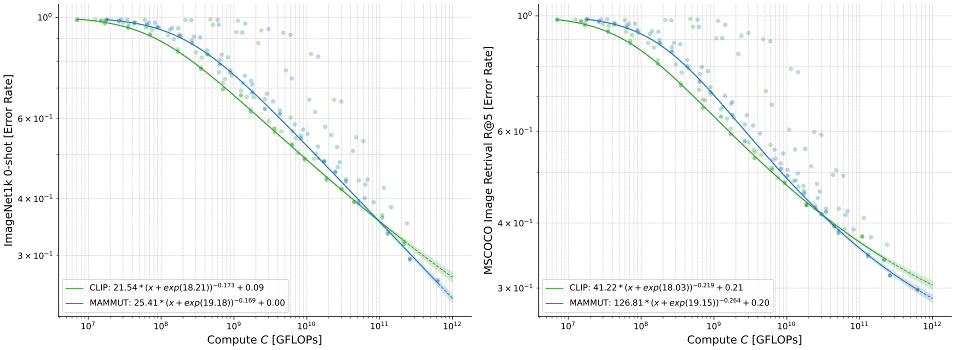

(a) ImageNet-1k 0-shot classification

(b) MS-COCO image R@5

Figure 2: **Scaling on Re-LAION-1.4B.** Comparison of CLIP and MaMMUT via scaling laws on Re-LAION-1.4B. Error rate on downstream tasks is plotted against compute. MaMMUT outperforms CLIP in terms of scalability, showing similar trends as in DataComp-1.4B.

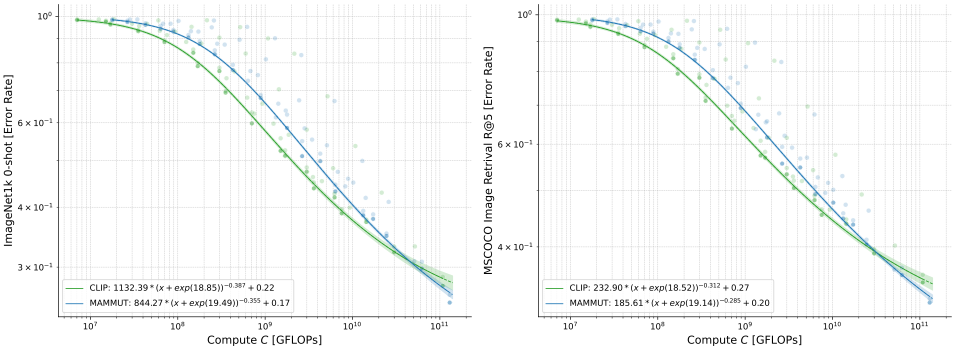

(a) ImageNet-1k 0-shot classification

(b) MS-COCO image R@5

Figure 3: **Scaling on DFN-1.4B.** Comparison of CLIP and MaMMUT via scaling laws on DFN-1.4B. Error rate on downstream tasks is plotted against compute. MaMMUT outperforms CLIP in terms of scalability, indicated by crossing scaling law fit lines, where MaMMUT takes over CLIP in performance from larger compute close to 10^{11} GFLOPS on, again showing similar trend as observed on DataComp and Re-LAION.

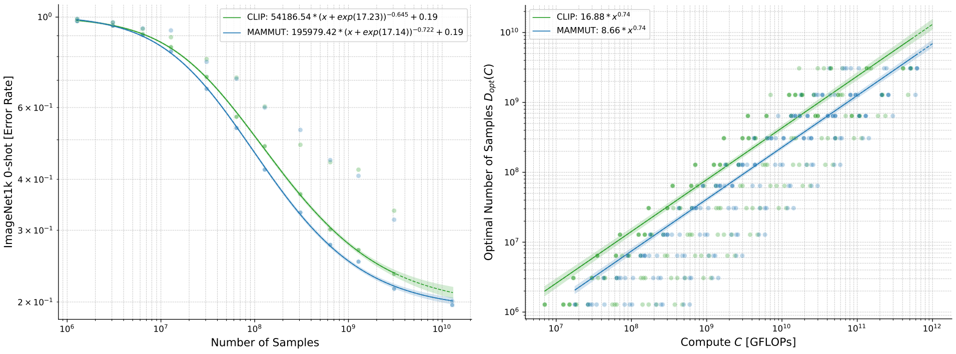

(a) IN-1k 0-Shot classification error rate vs. training dataset size

(b) Compute optimal dataset size $D_{opt}(C)$

Figure 4: Comparison of data efficiency and optimal dataset size for CLIP and MaMMUT via scaling laws on DataComp-1.4B. MaMMUT is more data efficient and requires smaller dataset size to be compute optimal.

MaMMUT makes **more effective use of training data** than CLIP. Therefore, these trends suggest that MaMMUT generalizes better and scales more favorably with additional data. Additionally, we derive scaling laws with respect to number of training samples on two other datasets - Re-LAION-1.4B and DFN-1.4B. In Fig. 11 we show that **MaMMUT shows consistently superior data efficiency across different training datasets** compared to CLIP. We also provide estimations for optimal number of training samples for unseen compute scales (see Tab. 2) for CLIP and MaMMUT trained on DataComp-1.4B. We use the predicted compute-optimal number of samples to estimate IN1k classification error rate using obtained power fit following Eq. 2 (see Fig. 4). We see that MaMMUT is a more scalable model which agrees with estimation obtained from fitting Eq. 1 on the experimental data (see Fig. 1 and Tab. 9).

GFLOPs	Predicted $D_{\text{opt}}(C)$ (95% CI)	Model Candidate	#Params	Predicted IN1k 0-shot acc (95% CI)
2.14e+12	2.30e+10 (2.75e+10, 1.91e+10)	ViT-SO150M-14-smaller-text	279M	0.794 (0.785, 0.803)
2.59e+12	2.64e+10 (3.19e+10, 2.20e+10)	ViT-SO150M-14-smaller-text	295M	0.795 (0.786, 0.804)
2.14e+12	1.23e+10 (1.39e+10, 1.09e+10)	mammut-ViT-L-14	522M	0.798 (0.794, 0.803)
2.59e+12	1.42e+10 (1.61e+10, 1.25e+10)	mammut-ViT-L-14	548M	0.799 (0.795, 0.804)

Table 2: Predicted compute optimal samples seen and accuracy for each compute budget and model configuration, with parameter sizes annotated in millions (M).

3.3 Scaling law derivation using constant learning rate scheduler

We follow [42] and show a scaling law derivation based on training with constant learning rate, thus saving 98% of compute compared to cosine. We omit points from warmup duration in our derivation, to prevent noise in the low-compute part of the scaling law. In Fig. 5 we visualize our results, showing the measurements density and in Tab. 6 we tabulate the coefficients. Our results further support the better scalability of MaMMUT over CLIP, showing consistent trends even when replacing learning rate scheduler.

3.4 Comparison via scaling law for fine-tuning error on segmentation dense prediction task

For further comparison evidence, we derive a scaling law (Eq. 1) for ADE20K segmentation error $(1 - \text{mIoU})$ after fine-tuning dependent on pre-training compute scale for CLIP and MaMMUT. As shown in Fig. 6, MaMMUT again exhibits stronger scaling than CLIP ($\alpha = 0.208$ vs. 0.354), with an error crossover at approximately 10^9 GFLOPs. This is far below the crossover at approximately 10^{11} GFLOPs observed for zero-shot ImageNet classification (Fig. 1a), indicating that captioning supervision via fine-tuning improves dense prediction already at lower pre-training scales. See more details in Appendix H.

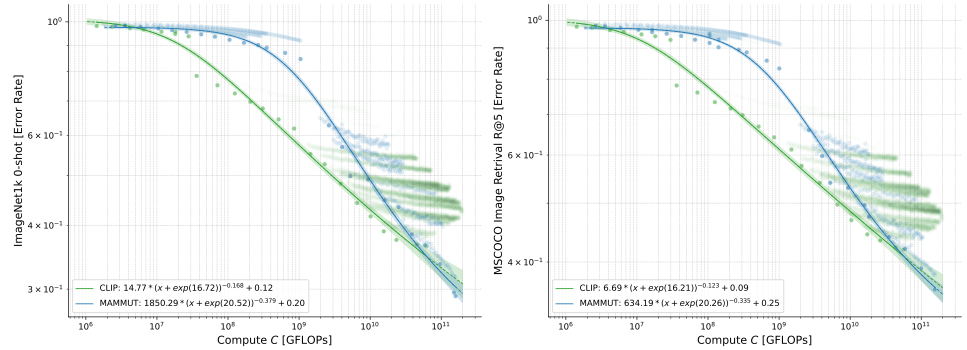

(a) ImageNet-1k 0-shot classification

(b) MS-COCO image R@5

Figure 5: **Scaling law fits using constant learning rate scheduler.** Comparison of CLIP and MaMMUT via scaling laws on DataComp-1.4B. Error rate on downstream tasks is plotted against compute. Using constant learning rate scheduler for scaling law derivation reveals the same trend as with cosine - MaMMUT outperforms CLIP in terms of scalability.

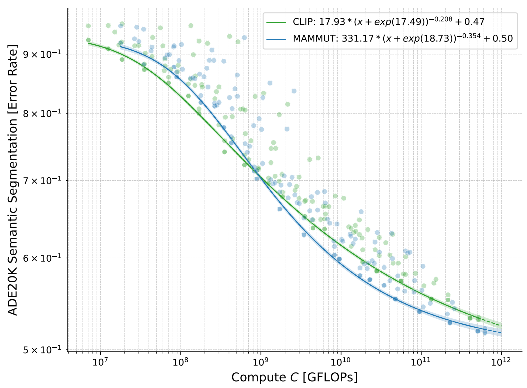

Figure 6: **Scaling law for semantic segmentation.** Downstream error rate (1 – mIoU) of openCLIP and openMaMMUT pre-trained on DataComp-1.4B and fine-tuned on ADE20K. MaMMUT shows higher performance than CLIP for segmentation at higher scales.

3.5 Scaling up following the comparison: OpenMaMMUT-L-14

We used insights and predictions from our scaling analysis and comparisons to train OpenMaMMUT-L-14, a large scale open vision-language foundation model. We chose to train on 12.8B samples of DataComp-1.4B to have direct comparison to openCLIP trained in previous work [19]. More info on training hyperparameters can be found in Tab. 11. OpenMaMMUT achieves **state of the art performance** on zero-shot classification and retrieval tasks among similar-sized models trained only on publicly-available data (MetaCLIP, DataComp, OpenVision, Tab. 3). It outperforms with 80.3% IN1k accuracy as predicted openCLIP pre-trained on same DataComp-1.4B budget of 12.8B (79.2%) and even rivals models with much larger pre-training compute like SigLIP. OpenMaMMUT represents a highly performant, fully reproducible alternative to other models with **openly available data and training code**. Note that on 12.8B samples seen scale the performance suffers from high amount of repetitions, and therefore is below our prediction of 82% (Tab. 1) that is valid for training on unique samples.

4 Related work & limitations

Recent work has investigated the performance of vision-language models such as CLIP [7], CoCa [16], MaMMUT [17], Cap [45], SigLIP [14], TULIP[46] or OpenVision[47] at various scales. These studies analyze different model sizes and highlight either architectural or dataset innovations;

						ImageNet-1k		COCO	
ViT	Res.	Seq.	Model	Dataset	#Samples	val	v2	T→I	I→T
L/16	256	256	SigLIP [18]	WebLI-10B	40B	80.44	73.76	75.26	88.40
			SigLIP 2 [14]	WebLI-10B	40B	82.35	76.66	76.84	90.44
L/14	224	256	OpenCLIP [10]	LAION-2B	34B	75.24	67.73	70.46	84.30
			CLIP [7]	WIT-400M	12.8B	75.54	69.84	59.95	79.56
			MetaCLIP [43]	MetaCLIP-2.5B	12.8B	79.19	72.64	71.36	84.94
			EVA-CLIP [44]	Merged-2B	4B*	79.75*	72.92*	70.68	85.26
			DFN [20]	DFN-2B	13B	**81.41***	**74.58***	**73.19***	**86.20***
			DataComp [19]	DataComp-1.4B	12.8B	79.19	72.06	69.86	84.64
			OpenMaMMUT (Ours)	DataComp-1.4B	12.8B	80.34	73.78	71.19	85.88

Table 3: Zero-shot classification (accuracy) and retrieval (R@5) results. DFN used ImageNet/MS-COCO-finetuned model for data filtering; EVA-CLIP was initialized from models pre-trained on ImageNet. We use **bold** for best overall results, gray for models involving ImageNet/MS-COCO data as training data in pipeline, and underlined for best results without ImageNet/MS-COCO involvement.

however, they do not perform a comprehensive scaling law analysis. Furthermore, the datasets used in these works—such as WIT for OpenAI CLIP and WebLI for SigLIP—are **closed**, severely limiting reproducibility and making it impossible to study which of algorithmic or dataset interventions claimed to have beneficial effect on learning used in those studies indeed lead to better model performance. In App. Fig. 12, we compare open implementations of CoCa and SigLIP to openCLIP on DataComp-1.4B, finding no significant difference of SigLIP to standard CLIP in model scalability.

In [48], authors investigate how various language model families compare in terms of their scaling behavior. While it offers valuable insights into architectural trends, it does not use for comparison a full scaling law framework in the sense of jointly modeling loss or downstream task performance as a function of compute and dataset size varied systematically across multiple scales. As accuracy of predictions derived from such trends was not measured, it makes it unclear whether observed trends for various language model architectures are to be trusted and whether comparison would remain valid across various scenarios, which we demonstrate to be the case for scaling law based comparison.

Preparing grounds for this work, [10] derived first reproducible scaling laws for openCLIP using LAION datasets and performed comparison between open LAION-400M/5B and closed WIT. The work used however only few samples seen scales, while also going up to scales that are prone to strongly diminishing performance due to heavy sample repetition (6x on 12.8B and 17x on 34B sample seen scales). This affects extrapolations of the scaling law and thus the validity of comparisons based on it. Interestingly, in our work using much denser scaling law derivation without strong repetitions for higher prediction accuracy, we can confirm the dataset comparison in [10] using Re-LAION-1.4B, observing same trends for WIT being better on zero-shot classification (App. Fig. 7) while worse on retrieval (App. Fig. 8), providing further evidence for robustness of scaling law based comparison. Another data-centric work responsible for composing open DataComp-1.4B dataset [19] used measurements on few selected scales to compare datasets and decide for benefit of various dataset interventions. No scaling laws were derived to back up the comparisons, leaving unclear whether the observed trends will propagate across larger scales than taken for the comparisons.

Several works explored the effects of data constraints on scaling laws. Notably, studies investigating the scaling law behavior under dataset repetitions for language models [38, 41] and for CLIP[49] reported that high repetition factors can lead to heavily diminished performance compared to the Pareto front of scaling with unique data samples. Our experiments carefully limit the repetition factor to less than $3\times$, minimizing such confounding effects, assuming unique samples or only little sample repetition for comparisons to be valid on Pareto front with strong performance scaling.

Building on these foundations, our work provides a unified and empirically grounded scaling law analysis of vision-language models trained on open datasets. We explicitly model performance as a function of data and compute [8, 9], and compare multiple architectures under fully controlled, consistent and reproducible settings. Unlike prior work, our approach enables rigorous comparison of both data and compute efficiency, ensuring the consistency of the comparison across scales and training conditions.

Limitations. While our work provides a comprehensive analysis for language-vision models such as CLIP and MaMMUT trained on large-scale open foundation datasets, it also has several limitations:

1) We mostly use zero-shot setting for model evaluation (for classification and retrieval tasks), using fine-tuning only for segmentation. Linear probing, fine-tuning [10] or vision instruction-tuning [12] of the pre-trained vision encoders can provide further insights into validity and consistency of scaling laws based comparison. **2)** While open datasets we use have substantial scale - 1.4B unique samples - this still limits the ability of derived scaling laws to extrapolate to higher scales, as the effect of sample repetition has to be considered when conducting measurements above 1.4B. To test comparison validity and scaling law predictions on larger reference scales like 12.8B, larger scale open datasets are required. **3)** In our study we only looked at standard contrastive loss or contrastive and captioning loss objectives and did not incorporate further "loss mixtures" such as masking or diffusion-based losses. We also did not derive scaling laws for specific architectural components such as optimal number of parameters in text or vision tower, or other important properties of training procedure like image input resolution and patch size, or context length in general. In its current form, scaling laws based comparison has high computational cost, prohibiting naive incorporation of many factors that influence scalability of the training procedure.

5 Discussion & conclusion

In this work, we show how systematic learning procedure comparison can be performed via scaling law derivation under fully controlled, reproducible training conditions when using open foundation models and open datasets. We take as example scenario openCLIP [7, 22, 10] and openMaMMUT based on [17], two important open language-vision models relying either on image-text contrastive only or contrastive and captioning loss, trained on three important open reference datasets, DataComp-1.4B [19], Re-LAION-1.4B [21] and DFN-1.4B [20]. We show that deriving scaling laws gives comparison of model and dataset based on their estimated scalability for wide scale spans and for various downstream tasks, aligned on same total pre-training compute. Such comparison can be validated by checking consistency of scaling trends in different scenarios. For instance, openMaMMUT scalability is stronger than openCLIP both on zero-shot classification and retrieval, also showing advantage for a wide scale span on segmentation, and across all three open datasets. Also, inconsistencies are insightful - for instance, DataComp-1.4B shows stronger scalability for both openMaMMUT and openCLIP for zero-shot classification while being slightly weaker for retrieval. Thus, none of these two datasets is the most scalable candidate across all downstream tasks, and scaling advantage there is task dependent. DFN on the other hand is consistently better than other datasets across downstream tasks and for both openMaMMUT and openCLIP.

Comparison via scaling laws offers better protection against misleading conclusions derived from comparison of only few selected points, especially when done on small scales only. On smaller scales, openCLIP outperforms stronger scalable openMaMMUT that takes over on larger scales. Remarkably, we observe the compute scale threshold where openMaMMUT takes over openCLIP to be consistently settled between 10^{10} and 10^{11} GFLOPS across datasets, zero-shot downstream tasks and learning schedules. This gives further evidence for the robustness of scaling law based comparison. To properly estimate such crossings, it is crucial to perform dense measurements on smaller scales and use fitting routines that allow for accurate extrapolation to larger scales. Efficient derivation of accurate scaling laws [42, 11] to determine factors affecting scalability of the learning procedure is thus an important topic for future work.

In our study, we used open datasets with 1.4B samples. While this is sufficient to demonstrate usefulness of scaling law based comparison, more accurate predictions for training at larger scales on unique samples require larger datasets. Those are also required to train larger scale models with predicted strong capabilities, as too many repetitions on smaller datasets might lead to diminished performance [41, 49], which we see in openMaMMUT L-14 trained on 12.8B samples, staying with zero-shot IN1k 80.3% below the predicted 82% (Tab. 1). Deriving scaling law correction for diminishing performance due to data repetitions as well as increasing scale of open datasets are important directions for future work.

While we show that robust and reproducible comparison via scaling law derivation is possible, it relies crucially on the whole pipeline to be fully open - including dataset composition, training itself, and downstream evaluation. We hope that our work will encourage the creation of more open artefacts, especially open datasets as those are still scarce [50, 19, 20, 21], to enable collaborative and reproducible progress towards stronger scalable open foundation models guided by independently verifiable and systematic comparison.

Acknowledgements

MN, TP, MC and JJ acknowledge funding by the Federal Ministry of Education and Research of Germany (BMBF) under grant no. 01IS24085C (OPENHAFM), under the grant 16HPC117K (MINERVA) and under the grant no. 01IS22094B (WestAI - AI Service Center West), as well as funding by EU Horizon under grant no. 101214398 (ELLIOT) and co-funding by EU from EuroHPC Joint Undertaking programm under grant no. 101182737 (MINERVA) and from Digital Europe Programme under grant no. 101195233 (openEuroLLM).

Giovanni Puccetti is fully funded by the project "Italian Strengthening of ESFRI RI RESILIENCE" (ITSERR) funded by the European Union under the NextGenerationEU funding scheme (CUP:B53C22001770006).

We gratefully acknowledge the Gauss Centre for Supercomputing e.V. for funding this work by providing computing time through the John von Neumann Institute for Computing (NIC) on the supercomputer JUWELS Booster at Jülich Supercomputing Centre (JSC), EuroHPC Joint Undertaking for computing time and storage on the EuroHPC supercomputer LEONARDO, hosted by CINECA (Italy) and the LEONARDO consortium through an EuroHPC Extreme Access grant EHPC-EXT-2023E02-068 and in part by Iscra B Project REWATCH (Project Number: HP10BL323R), storage resources on JUST granted and operated by JSC and supported by Helmholtz Data Federation (HDF), computing time granted by the JARA and JSC on the supercomputer JURECA at JSC, and computing time granted on prototype JEDI via JUREAP (JUPITER Early Access Programm) grant at JSC. LAION further acknowledges storage grant by HuggingFace that allows us to provide convenient access to the output of the open-source research to broad community via HF repository.

Further thanks go for support provided by supercomputing facilities and their teams, especially to Damian Alvarez and Mathis Bode from Juelich Supercomputer Center (JSC, Germany) and to Laura Morselli from CINECA (Italy).

We also would like to express gratitude to all the people who are working on making code, models and data publicly available, advancing community based research and making research more reproducible. Specifically, we would like to thank all the members of the LAION Discord server[2] community and Open-Ψ (Open-Sci) Collective[3] for providing fruitful ground for scientific exchange and open-source development.

References

[1] Rishi Bommasani, Drew A Hudson, Ehsan Adeli, Russ Altman, Simran Arora, Sydney von Arx, Michael S Bernstein, Jeannette Bohg, Antoine Bosselut, Emma Brunskill, et al. On the opportunities and risks of foundation models. *arXiv preprint arXiv:2108.07258*, 2021.

[2] Jacob Devlin, Ming-Wei Chang, Kenton Lee, and Kristina Toutanova. Bert: Pre-training of deep bidirectional transformers for language understanding. *arXiv preprint arXiv:1810.04805*, 2018.

[3] Colin Raffel, Noam Shazeer, Adam Roberts, Katherine Lee, Sharan Narang, Michael Matena, Yanqi Zhou, Wei Li, and Peter J Liu. Exploring the limits of transfer learning with a unified text-to-text transformer. *Journal of machine learning research*, 21(140):1–67, 2020.

[4] Tom Brown, Benjamin Mann, Nick Ryder, Melanie Subbiah, Jared D Kaplan, Prafulla Dhariwal, Arvind Neelakantan, Pranav Shyam, Girish Sastry, Amanda Askell, et al. Language models are few-shot learners. *Advances in neural information processing systems*, 33:1877–1901, 2020.

[5] David Fan, Shengbang Tong, Jiachen Zhu, Koustuv Sinha, Zhuang Liu, Xinlei Chen, Michael Rabbat, Nicolas Ballas, Yann LeCun, Amir Bar, et al. Scaling language-free visual representation learning. *arXiv preprint arXiv:2504.01017*, 2025.

[6] Benjamin Elizalde, Soham Deshmukh, Mahmoud Al Ismail, and Huaming Wang. Clap learning audio concepts from natural language supervision. In *ICASSP 2023-2023 IEEE International Conference on Acoustics, Speech and Signal Processing (ICASSP)*, pages 1–5. IEEE, 2023.

[2] `https://discord.gg/BZqhreFazY`

[3] `https://discord.gg/GsKh4mBVcv`

[7] Alec Radford, Jong Wook Kim, Chris Hallacy, Aditya Ramesh, Gabriel Goh, Sandhini Agarwal, Girish Sastry, Amanda Askell, Pamela Mishkin, Jack Clark, et al. Learning transferable visual models from natural language supervision. In *International Conference on Machine Learning*, pages 8748–8763. PMLR, 2021.

[8] Jared Kaplan, Sam McCandlish, Tom Henighan, Tom B Brown, Benjamin Chess, Rewon Child, Scott Gray, Alec Radford, Jeffrey Wu, and Dario Amodei. Scaling laws for neural language models. *arXiv preprint arXiv:2001.08361*, 2020.

[9] Jordan Hoffmann, Sebastian Borgeaud, Arthur Mensch, Elena Buchatskaya, Trevor Cai, Eliza Rutherford, Diego de las Casas, Lisa Anne Hendricks, Johannes Welbl, Aidan Clark, Tom Hennigan, Eric Noland, Katherine Millican, George van den Driessche, Bogdan Damoc, Aurelia Guy, Simon Osindero, Karen Simonyan, Erich Elsen, Oriol Vinyals, Jack William Rae, and Laurent Sifre. An empirical analysis of compute-optimal large language model training. In Alice H. Oh, Alekh Agarwal, Danielle Belgrave, and Kyunghyun Cho, editors, *Advances in Neural Information Processing Systems*, 2022.

[10] Mehdi Cherti, Romain Beaumont, Ross Wightman, Mitchell Wortsman, Gabriel Ilharco, Cade Gordon, Christoph Schuhmann, Ludwig Schmidt, and Jenia Jitsev. Reproducible scaling laws for contrastive language-image learning. In *Proceedings of the IEEE/CVF conference on computer vision and pattern recognition*, pages 2818–2829, 2023.

[11] Margaret Li, Sneha Kudugunta, and Luke Zettlemoyer. (mis)fitting scaling laws: A survey of scaling law fitting techniques in deep learning. In *The Thirteenth International Conference on Learning Representations*, 2025.

[12] Haotian Liu, Chunyuan Li, Qingyang Wu, and Yong Jae Lee. Visual instruction tuning. *Advances in neural information processing systems*, 36:34892–34916, 2023.

[13] Zhe Chen, Jiannan Wu, Wenhai Wang, Weijie Su, Guo Chen, Sen Xing, Muyan Zhong, Qinglong Zhang, Xizhou Zhu, Lewei Lu, et al. Internvl: Scaling up vision foundation models and aligning for generic visual-linguistic tasks. In *Proceedings of the IEEE/CVF conference on computer vision and pattern recognition*, pages 24185–24198, 2024.

[14] Michael Tschannen, Alexey Gritsenko, Xiao Wang, Muhammad Ferjad Naeem, Ibrahim Alabdulmohsin, Nikhil Parthasarathy, Talfan Evans, Lucas Beyer, Ye Xia, Basil Mustafa, et al. Siglip 2: Multilingual vision-language encoders with improved semantic understanding, localization, and dense features. *arXiv preprint arXiv:2502.14786*, 2025.

[15] Dustin Podell, Zion English, Kyle Lacey, Andreas Blattmann, Tim Dockhorn, Jonas Müller, Joe Penna, and Robin Rombach. Sdxl: Improving latent diffusion models for high-resolution image synthesis. *arXiv preprint arXiv:2307.01952*, 2023.

[16] Jiahui Yu, Zirui Wang, Vijay Vasudevan, Legg Yeung, Mojtaba Seyedhosseini, and Yonghui Wu. Coca: Contrastive captioners are image-text foundation models. *arXiv preprint arXiv:2205.01917*, 2022.

[17] Weicheng Kuo, AJ Piergiovanni, Dahun Kim, xiyang luo, Benjamin Caine, Wei Li, Abhijit Ogale, Luowei Zhou, Andrew M. Dai, Zhifeng Chen, Claire Cui, and Anelia Angelova. MaMMUT: A simple architecture for joint learning for multimodal tasks. *Transactions on Machine Learning Research*, 2023.

[18] Xiaohua Zhai, Basil Mustafa, Alexander Kolesnikov, and Lucas Beyer. Sigmoid loss for language image pre-training. In *Proceedings of the IEEE/CVF international conference on computer vision*, pages 11975–11986, 2023.

[19] Samir Yitzhak Gadre, Gabriel Ilharco, Alex Fang, Jonathan Hayase, Georgios Smyrnis, Thao Nguyen, Ryan Marten, Mitchell Wortsman, Dhruba Ghosh, Jieyu Zhang, et al. Datacomp: In search of the next generation of multimodal datasets. *Advances in Neural Information Processing Systems*, 36:27092–27112, 2023.

[20] Alex Fang, Albin Madappally Jose, Amit Jain, Ludwig Schmidt, Alexander Toshev, and Vaishaal Shankar. Data filtering networks. In *The Twelfth International Conference on Learning Representations*, 2024.

[21] LAION. Releasing re-laion 5b: transparent iteration on laion-5b with additional safety fixes. `https://laion.ai/blog/relaion-5b/`, 2024. Accessed: 30 aug, 2024.

[22] G. Ilharco, M. Wortsman, N. Carlini, R. Taori, A. Dave, V. Shankar, H. Namkoong, J. Miller, H. Hajishirzi, A. Farhadi, and L. Schmidt. Openclip. 2021.

[23] Aaron van den Oord, Yazhe Li, and Oriol Vinyals. Representation learning with contrastive predictive coding. *arXiv preprint arXiv:1807.03748*, 2018.

[24] Ilya Loshchilov and Frank Hutter. Decoupled weight decay regularization. *arXiv preprint arXiv:1711.05101*, 2017.

[25] Melanie Mitchell. How do we know how smart ai systems are? *Science*, 381(6654):eadj5957, 2023.

[26] J. Deng, W. Dong, R. Socher, L. Li, Kai Li, and Li Fei-Fei. Imagenet: A large-scale hierarchical image database. In *Proc. IEEE Conf. Computer Vision and Pattern Recognition*, pages 248–255, June 2009.

[27] Benjamin Recht, Rebecca Roelofs, Ludwig Schmidt, and Vaishaal Shankar. Do imagenet classifiers generalize to imagenet? In *International conference on machine learning*, pages 5389–5400. PMLR, 2019.

[28] Dan Hendrycks, Steven Basart, Norman Mu, Saurav Kadavath, Frank Wang, Evan Dorundo, Rahul Desai, Tyler Zhu, Samyak Parajuli, Mike Guo, Dawn Song, Jacob Steinhardt, and Justin Gilmer. The many faces of robustness: A critical analysis of out-of-distribution generalization. *International Conference on Computer Vision (ICCV)*, 2021. `https://arxiv.org/abs/2006.16241`.

[29] Dan Hendrycks, Kevin Zhao, Steven Basart, Jacob Steinhardt, and Dawn Song. Natural adversarial examples. *Conference on Computer Vision and Pattern Recognition (CVPR)*, 2021. `https://arxiv.org/abs/1907.07174`.

[30] Haohan Wang, Songwei Ge, Zachary Lipton, and Eric P Xing. Learning robust global representations by penalizing local predictive power. In *Advances in Neural Information Processing Systems (NeurIPS)*, 2019. `https://arxiv.org/abs/1905.13549`.

[31] Andrei Barbu, David Mayo, Julian Alverio, William Luo, Christopher Wang, Dan Gutfreund, Josh Tenenbaum, and Boris Katz. Objectnet: A large-scale bias-controlled dataset for pushing the limits of object recognition models. In *Advances in Neural Information Processing Systems (NeurIPS)*, 2019.

[32] Romain Beaumont Mehdi Cherti et al. Clip benchmark. `https://github.com/LAION-AI/CLIP_benchmark`, 2023.

[33] Tsung-Yi Lin, Michael Maire, Serge Belongie, James Hays, Pietro Perona, Deva Ramanan, Piotr Dollár, and C Lawrence Zitnick. Microsoft coco: Common objects in context. In *European conference on computer vision*, pages 740–755. Springer, 2014.

[34] Bolei Zhou, Hang Zhao, Xavier Puig, Sanja Fidler, Adela Barriuso, and Antonio Torralba. Scene Parsing through ADE20K Dataset. In *Proceedings of the IEEE/CVF Conference on Computer Vision and Pattern Recognition (CVPR)*, pages 5122–5130, 2017.

[35] Tommie Kerssies, Daan De Geus, and Gijs Dubbelman. How to Benchmark Vision Foundation Models for Semantic Segmentation? In *Proceedings of the IEEE/CVF Conference on Computer Vision and Pattern Recognition (CVPR) Workshops*, pages 1162–1171, 2024.

[36] Tommie Kerssies, Niccolò Cavagnero, Alexander Hermans, Narges Norouzi, Giuseppe Averta, Bastian Leibe, Gijs Dubbelman, and Daan de Geus. Your ViT is Secretly an Image Segmentation Model. In *Proceedings of the IEEE/CVF Conference on Computer Vision and Pattern Recognition (CVPR)*, 2025.

[37] Xiaohua Zhai, Alexander Kolesnikov, Neil Houlsby, and Lucas Beyer. Scaling vision transformers. In *Proceedings of the IEEE/CVF conference on computer vision and pattern recognition*, pages 12104–12113, 2022.

[38] Tom Henighan, Jared Kaplan, Mor Katz, Mark Chen, Christopher Hesse, Jacob Jackson, Heewoo Jun, Tom B Brown, Prafulla Dhariwal, Scott Gray, et al. Scaling laws for autoregressive generative modeling. *arXiv preprint arXiv:2010.14701*, 2020.

[39] Jordan Hoffmann, Sebastian Borgeaud, Arthur Mensch, Elena Buchatskaya, Trevor Cai, Eliza Rutherford, Diego de Las Casas, Lisa Anne Hendricks, Johannes Welbl, Aidan Clark, et al. Training compute-optimal large language models. *arXiv preprint arXiv:2203.15556*, 2022.

[40] Stephan Borzsony, Donald Kossmann, and Konrad Stocker. The skyline operator. In *Proceedings 17th international conference on data engineering*, pages 421–430. IEEE, 2001.

[41] Niklas Muennighoff, Alexander Rush, Boaz Barak, Teven Le Scao, Nouamane Tazi, Aleksandra Piktus, Sampo Pyysalo, Thomas Wolf, and Colin A Raffel. Scaling data-constrained language models. *Advances in Neural Information Processing Systems*, 36:50358–50376, 2023.

[42] Tomer Porian, Mitchell Wortsman, Jenia Jitsev, Ludwig Schmidt, and Yair Carmon. Resolving discrepancies in compute-optimal scaling of language models. *Advances in Neural Information Processing Systems*, 37:100535–100570, 2024.

[43] Hu Xu, Saining Xie, Xiaoqing Ellen Tan, Po-Yao Huang, Russell Howes, Vasu Sharma, Shang-Wen Li, Gargi Ghosh, Luke Zettlemoyer, and Christoph Feichtenhofer. Demystifying clip data. *arXiv preprint arXiv:2309.16671*, 2023.

[44] Quan Sun, Yuxin Fang, Ledell Wu, Xinlong Wang, and Yue Cao. Eva-clip: Improved training techniques for clip at scale. *arXiv preprint arXiv:2303.15389*, 2023.

[45] Michael Tschannen, Manoj Kumar, Andreas Steiner, Xiaohua Zhai, Neil Houlsby, and Lucas Beyer. Image captioners are scalable vision learners too. *Advances in Neural Information Processing Systems*, 36:46830–46855, 2023.

[46] Zineng Tang, Long Lian, Seun Eisape, XuDong Wang, Roei Herzig, Adam Yala, Alane Suhr, Trevor Darrell, and David M Chan. Tulip: Towards unified language-image pretraining. *arXiv preprint arXiv:2503.15485*, 2025.

[47] Xianhang Li, Yanqing Liu, Haoqin Tu, Hongru Zhu, and Cihang Xie. Openvision: A fully-open, cost-effective family of advanced vision encoders for multimodal learning. *arXiv preprint arXiv:2505.04601*, 2025.

[48] Yi Tay, Mostafa Dehghani, Samira Abnar, Hyung Won Chung, William Fedus, Jinfeng Rao, Sharan Narang, Vinh Q Tran, Dani Yogatama, and Donald Metzler. Scaling laws vs model architectures: How does inductive bias influence scaling? *arXiv preprint arXiv:2207.10551*, 2022.

[49] Sachin Goyal, Pratyush Maini, Zachary C Lipton, Aditi Raghunathan, and J Zico Kolter. Scaling laws for data filtering–data curation cannot be compute agnostic. In *Proceedings of the IEEE/CVF Conference on Computer Vision and Pattern Recognition*, pages 22702–22711, 2024.

[50] Christoph Schuhmann, Romain Beaumont, Richard Vencu, Cade W Gordon, Ross Wightman, Mehdi Cherti, Theo Coombes, Aarush Katta, Clayton Mullis, Mitchell Wortsman, Patrick Schramowski, Srivatsa R Kundurthy, Katherine Crowson, Ludwig Schmidt, Robert Kaczmarczyk, and Jenia Jitsev. LAION-5B: An open large-scale dataset for training next generation image-text models. In *Thirty-sixth Conference on Neural Information Processing Systems (NeurIPS), Datasets and Benchmarks Track*, 2022.

NeurIPS Paper Checklist

1. **Claims**

   Question: Do the main claims made in the abstract and introduction accurately reflect the paper's contributions and scope?

   Answer: [Yes]

   Justification: Claims in the abstract are backed up by the experimental results described in the main paper results Section 3.

   Guidelines:

   - The answer NA means that the abstract and introduction do not include the claims made in the paper.
   - The abstract and/or introduction should clearly state the claims made, including the contributions made in the paper and important assumptions and limitations. A No or NA answer to this question will not be perceived well by the reviewers.
   - The claims made should match theoretical and experimental results, and reflect how much the results can be expected to generalize to other settings.
   - It is fine to include aspirational goals as motivation as long as it is clear that these goals are not attained by the paper.

2. **Limitations**

   Question: Does the paper discuss the limitations of the work performed by the authors?

   Answer: [Yes]

   Justification: see Section 4

   Guidelines:

   - The answer NA means that the paper has no limitation while the answer No means that the paper has limitations, but those are not discussed in the paper.
   - The authors are encouraged to create a separate "Limitations" section in their paper.
   - The paper should point out any strong assumptions and how robust the results are to violations of these assumptions (e.g., independence assumptions, noiseless settings, model well-specification, asymptotic approximations only holding locally). The authors should reflect on how these assumptions might be violated in practice and what the implications would be.
   - The authors should reflect on the scope of the claims made, e.g., if the approach was only tested on a few datasets or with a few runs. In general, empirical results often depend on implicit assumptions, which should be articulated.
   - The authors should reflect on the factors that influence the performance of the approach. For example, a facial recognition algorithm may perform poorly when image resolution is low or images are taken in low lighting. Or a speech-to-text system might not be used reliably to provide closed captions for online lectures because it fails to handle technical jargon.
   - The authors should discuss the computational efficiency of the proposed algorithms and how they scale with dataset size.
   - If applicable, the authors should discuss possible limitations of their approach to address problems of privacy and fairness.
   - While the authors might fear that complete honesty about limitations might be used by reviewers as grounds for rejection, a worse outcome might be that reviewers discover limitations that aren't acknowledged in the paper. The authors should use their best judgment and recognize that individual actions in favor of transparency play an important role in developing norms that preserve the integrity of the community. Reviewers will be specifically instructed to not penalize honesty concerning limitations.

3. **Theory assumptions and proofs**

   Question: For each theoretical result, does the paper provide the full set of assumptions and a complete (and correct) proof?

   Answer: [NA]

Justification: There are no theoretical results in the paper.

Guidelines:

- The answer NA means that the paper does not include theoretical results.
- All the theorems, formulas, and proofs in the paper should be numbered and cross-referenced.
- All assumptions should be clearly stated or referenced in the statement of any theorems.
- The proofs can either appear in the main paper or the supplemental material, but if they appear in the supplemental material, the authors are encouraged to provide a short proof sketch to provide intuition.
- Inversely, any informal proof provided in the core of the paper should be complemented by formal proofs provided in appendix or supplemental material.
- Theorems and Lemmas that the proof relies upon should be properly referenced.

4. **Experimental result reproducibility**

   Question: Does the paper fully disclose all the information needed to reproduce the main experimental results of the paper to the extent that it affects the main claims and/or conclusions of the paper (regardless of whether the code and data are provided or not)?

   Answer: [Yes]

   Justification: Paper works with publicly available open datasets, will provide open-source code and data obtained from experiments to reproduce the results.

   Guidelines:

   - The answer NA means that the paper does not include experiments.
   - If the paper includes experiments, a No answer to this question will not be perceived well by the reviewers: Making the paper reproducible is important, regardless of whether the code and data are provided or not.
   - If the contribution is a dataset and/or model, the authors should describe the steps taken to make their results reproducible or verifiable.
   - Depending on the contribution, reproducibility can be accomplished in various ways. For example, if the contribution is a novel architecture, describing the architecture fully might suffice, or if the contribution is a specific model and empirical evaluation, it may be necessary to either make it possible for others to replicate the model with the same dataset, or provide access to the model. In general. releasing code and data is often one good way to accomplish this, but reproducibility can also be provided via detailed instructions for how to replicate the results, access to a hosted model (e.g., in the case of a large language model), releasing of a model checkpoint, or other means that are appropriate to the research performed.
   - While NeurIPS does not require releasing code, the conference does require all submissions to provide some reasonable avenue for reproducibility, which may depend on the nature of the contribution. For example
     (a) If the contribution is primarily a new algorithm, the paper should make it clear how to reproduce that algorithm.
     (b) If the contribution is primarily a new model architecture, the paper should describe the architecture clearly and fully.
     (c) If the contribution is a new model (e.g., a large language model), then there should either be a way to access this model for reproducing the results or a way to reproduce the model (e.g., with an open-source dataset or instructions for how to construct the dataset).
     (d) We recognize that reproducibility may be tricky in some cases, in which case authors are welcome to describe the particular way they provide for reproducibility. In the case of closed-source models, it may be that access to the model is limited in some way (e.g., to registered users), but it should be possible for other researchers to have some path to reproducing or verifying the results.

5. **Open access to data and code**

   Question: Does the paper provide open access to the data and code, with sufficient instructions to faithfully reproduce the main experimental results, as described in supplemental material?

Answer: [Yes]

Justification: Paper works with publicly available open datasets, will provide open-source code and data obtained from experiments to reproduce the results.

Guidelines:

- The answer NA means that paper does not include experiments requiring code.
- Please see the NeurIPS code and data submission guidelines (`https://nips.cc/public/guides/CodeSubmissionPolicy`) for more details.
- While we encourage the release of code and data, we understand that this might not be possible, so "No" is an acceptable answer. Papers cannot be rejected simply for not including code, unless this is central to the contribution (e.g., for a new open-source benchmark).
- The instructions should contain the exact command and environment needed to run to reproduce the results. See the NeurIPS code and data submission guidelines (`https://nips.cc/public/guides/CodeSubmissionPolicy`) for more details.
- The authors should provide instructions on data access and preparation, including how to access the raw data, preprocessed data, intermediate data, and generated data, etc.
- The authors should provide scripts to reproduce all experimental results for the new proposed method and baselines. If only a subset of experiments are reproducible, they should state which ones are omitted from the script and why.
- At submission time, to preserve anonymity, the authors should release anonymized versions (if applicable).
- Providing as much information as possible in supplemental material (appended to the paper) is recommended, but including URLs to data and code is permitted.

6. **Experimental setting/details**

   Question: Does the paper specify all the training and test details (e.g., data splits, hyperparameters, how they were chosen, type of optimizer, etc.) necessary to understand the results?

   Answer: [Yes]

   Justification: Paper contains all details necessary to understand the results, works with publicly available open data and will provide open-source code enabling researchers to reproduce the results.

   Guidelines:

   - The answer NA means that the paper does not include experiments.
   - The experimental setting should be presented in the core of the paper to a level of detail that is necessary to appreciate the results and make sense of them.
   - The full details can be provided either with the code, in appendix, or as supplemental material.

7. **Experiment statistical significance**

   Question: Does the paper report error bars suitably and correctly defined or other appropriate information about the statistical significance of the experiments?

   Answer: [Yes]

   Justification: Accuracy of scaling law prediction is estimated via confidence interval as described in in Section 2.4 and reported in Tab. 1 and Tab. 2

   Guidelines:

   - The answer NA means that the paper does not include experiments.
   - The authors should answer "Yes" if the results are accompanied by error bars, confidence intervals, or statistical significance tests, at least for the experiments that support the main claims of the paper.
   - The factors of variability that the error bars are capturing should be clearly stated (for example, train/test split, initialization, random drawing of some parameter, or overall run with given experimental conditions).

- The method for calculating the error bars should be explained (closed form formula, call to a library function, bootstrap, etc.)
- The assumptions made should be given (e.g., Normally distributed errors).
- It should be clear whether the error bar is the standard deviation or the standard error of the mean.
- It is OK to report 1-sigma error bars, but one should state it. The authors should preferably report a 2-sigma error bar than state that they have a 96% CI, if the hypothesis of Normality of errors is not verified.
- For asymmetric distributions, the authors should be careful not to show in tables or figures symmetric error bars that would yield results that are out of range (e.g. negative error rates).
- If error bars are reported in tables or plots, The authors should explain in the text how they were calculated and reference the corresponding figures or tables in the text.

8. **Experiments compute resources**

   Question: For each experiment, does the paper provide sufficient information on the computer resources (type of compute workers, memory, time of execution) needed to reproduce the experiments?

   Answer: [Yes]

   Justification: Paper provides information about compute spent for experiments, open-source code and data that will be released will contain information about exact configuration for performed trainings

   Guidelines:

   - The answer NA means that the paper does not include experiments.
   - The paper should indicate the type of compute workers CPU or GPU, internal cluster, or cloud provider, including relevant memory and storage.
   - The paper should provide the amount of compute required for each of the individual experimental runs as well as estimate the total compute.
   - The paper should disclose whether the full research project required more compute than the experiments reported in the paper (e.g., preliminary or failed experiments that didn't make it into the paper).

9. **Code of ethics**

   Question: Does the research conducted in the paper conform, in every respect, with the NeurIPS Code of Ethics `https://neurips.cc/public/EthicsGuidelines`?

   Answer: [Yes]

   Justification: The authors have reviewed the NeurIPS Code of Ethics and believe that the research conducted in the paper conforms to it.

   Guidelines:

   - The answer NA means that the authors have not reviewed the NeurIPS Code of Ethics.
   - If the authors answer No, they should explain the special circumstances that require a deviation from the Code of Ethics.
   - The authors should make sure to preserve anonymity (e.g., if there is a special consideration due to laws or regulations in their jurisdiction).

10. **Broader impacts**

    Question: Does the paper discuss both potential positive societal impacts and negative societal impacts of the work performed?

    Answer: [NA]

    Justification: There are no societal impacts of the work performed.

    Guidelines:

    - The answer NA means that there is no societal impact of the work performed.
    - If the authors answer NA or No, they should explain why their work has no societal impact or why the paper does not address societal impact.

- Examples of negative societal impacts include potential malicious or unintended uses (e.g., disinformation, generating fake profiles, surveillance), fairness considerations (e.g., deployment of technologies that could make decisions that unfairly impact specific groups), privacy considerations, and security considerations.
- The conference expects that many papers will be foundational research and not tied to particular applications, let alone deployments. However, if there is a direct path to any negative applications, the authors should point it out. For example, it is legitimate to point out that an improvement in the quality of generative models could be used to generate deepfakes for disinformation. On the other hand, it is not needed to point out that a generic algorithm for optimizing neural networks could enable people to train models that generate Deepfakes faster.
- The authors should consider possible harms that could arise when the technology is being used as intended and functioning correctly, harms that could arise when the technology is being used as intended but gives incorrect results, and harms following from (intentional or unintentional) misuse of the technology.
- If there are negative societal impacts, the authors could also discuss possible mitigation strategies (e.g., gated release of models, providing defenses in addition to attacks, mechanisms for monitoring misuse, mechanisms to monitor how a system learns from feedback over time, improving the efficiency and accessibility of ML).

11. **Safeguards**

    Question: Does the paper describe safeguards that have been put in place for responsible release of data or models that have a high risk for misuse (e.g., pre-trained language models, image generators, or scraped datasets)?

    Answer: [NA]

    Justification: The paper does not release data or models that have a high risk for misuse.

    Guidelines:

    - The answer NA means that the paper poses no such risks.
    - Released models that have a high risk for misuse or dual-use should be released with necessary safeguards to allow for controlled use of the model, for example by requiring that users adhere to usage guidelines or restrictions to access the model or implementing safety filters.
    - Datasets that have been scraped from the Internet could pose safety risks. The authors should describe how they avoided releasing unsafe images.
    - We recognize that providing effective safeguards is challenging, and many papers do not require this, but we encourage authors to take this into account and make a best faith effort.

12. **Licenses for existing assets**

    Question: Are the creators or original owners of assets (e.g., code, data, models), used in the paper, properly credited and are the license and terms of use explicitly mentioned and properly respected?

    Answer: [Yes]

    Justification: The resources used in the paper are properly credited and the license and terms of use are explicitly mentioned and respected.

    Guidelines:

    - The answer NA means that the paper does not use existing assets.
    - The authors should cite the original paper that produced the code package or dataset.
    - The authors should state which version of the asset is used and, if possible, include a URL.
    - The name of the license (e.g., CC-BY 4.0) should be included for each asset.
    - For scraped data from a particular source (e.g., website), the copyright and terms of service of that source should be provided.

- If assets are released, the license, copyright information, and terms of use in the package should be provided. For popular datasets, `paperswithcode.com/datasets` has curated licenses for some datasets. Their licensing guide can help determine the license of a dataset.
- For existing datasets that are re-packaged, both the original license and the license of the derived asset (if it has changed) should be provided.
- If this information is not available online, the authors are encouraged to reach out to the asset's creators.

13. **New assets**

    Question: Are new assets introduced in the paper well documented and is the documentation provided alongside the assets?

    Answer: [Yes]

    Justification: All assets are properly documented in the paper and will be described in the opne-source repo or at the corresponding HF location.

    Guidelines:

    - The answer NA means that the paper does not release new assets.
    - Researchers should communicate the details of the dataset/code/model as part of their submissions via structured templates. This includes details about training, license, limitations, etc.
    - The paper should discuss whether and how consent was obtained from people whose asset is used.
    - At submission time, remember to anonymize your assets (if applicable). You can either create an anonymized URL or include an anonymized zip file.

14. **Crowdsourcing and research with human subjects**

    Question: For crowdsourcing experiments and research with human subjects, does the paper include the full text of instructions given to participants and screenshots, if applicable, as well as details about compensation (if any)?

    Answer: [NA]

    Justification: The paper does not involve crowdsourcing nor research with human subjects.

    Guidelines:

    - The answer NA means that the paper does not involve crowdsourcing nor research with human subjects.
    - Including this information in the supplemental material is fine, but if the main contribution of the paper involves human subjects, then as much detail as possible should be included in the main paper.
    - According to the NeurIPS Code of Ethics, workers involved in data collection, curation, or other labor should be paid at least the minimum wage in the country of the data collector.

15. **Institutional review board (IRB) approvals or equivalent for research with human subjects**

    Question: Does the paper describe potential risks incurred by study participants, whether such risks were disclosed to the subjects, and whether Institutional Review Board (IRB) approvals (or an equivalent approval/review based on the requirements of your country or institution) were obtained?

    Answer: [NA]

    Justification: The paper does not involve crowdsourcing nor research with human subjects.

    Guidelines:

    - The answer NA means that the paper does not involve crowdsourcing nor research with human subjects.
    - Depending on the country in which research is conducted, IRB approval (or equivalent) may be required for any human subjects research. If you obtained IRB approval, you should clearly state this in the paper.

- We recognize that the procedures for this may vary significantly between institutions and locations, and we expect authors to adhere to the NeurIPS Code of Ethics and the guidelines for their institution.
- For initial submissions, do not include any information that would break anonymity (if applicable), such as the institution conducting the review.

16. **Declaration of LLM usage**

    Question: Does the paper describe the usage of LLMs if it is an important, original, or non-standard component of the core methods in this research? Note that if the LLM is used only for writing, editing, or formatting purposes and does not impact the core methodology, scientific rigorousness, or originality of the research, declaration is not required.

    Answer: [NA]

    Justification: LLMs were not used for conducting this research.

    Guidelines:

    - The answer NA means that the core method development in this research does not involve LLMs as any important, original, or non-standard components.
    - Please refer to our LLM policy (`https://neurips.cc/Conferences/2025/LLM`) for what should or should not be described.

Appendix: Scaling Laws for Comparison of Open Foundation Language-Vision Models and Datasets

A Estimated parameters for scaling law fits

To complement main results for scaling law based comparison of CLIP and MaMMUT (Sec. 3.1, Fig. 1, 2), we provide exact numbers of scaling law fits for both openCLIP and openMaMMUT measurements on zero shot IN1K classification and MS-COCO retrieval downstream tasks (Tab. 5a). Estimated values of exponents in power laws alone do not tell which models are more scalable, as we use here the functional form with additive terms for both irreducible error and non-zero random model performance (Eq. 1). Apart from plot visualization attesting Mammut stronger scalability than CLIP (Fig. 1, 2), scalability can be also compared via computing derivatives of the obtained fit in selected compute points. Derivatives that have larger absolute values stand for larger slope (bigger rate of decrease) and thus indicate stronger scalability. In Tab. 5b we show derivatives computed for scaling law fits, obtaining larger derivatives for openMaMMUT than for openCLIP, confirming again stronger scalability for MaMMUT over CLIP.

B More details on scaling law derivation experiments

Compute budget and energy consumption for the experiments. In Tab. 4, we provide overview over the GPU hours and energy spent for scaling law derivation experiments. We provide separate calculation for different learning rate schedule types (cosine, constant learning rate and constant learning rate + cooldown), for different datasets (Re-LAION-1.4B and DataComp-1.4B) and for different GPU types (A100 and H100). Large fraction of resources was spent for reference cosine schedule based scaling law derivation on DataComp-1.4B. We see that despite higher density of possible measurements, const based schedules use substantially less compute.

Detailed versions of scaling law plots. In the more detailed versions of scaling law plots (Fig. 16 and 17) we see the separate scaling curves for each model size (cooler colors indicate smaller models). The **bigger models require larger sample seen scale** to unfold their performance advantage, with the performance lagging behind smaller scale models on same smaller compute scale, where larger models suffer from sample seen scale bottleneck. On the other hand, **for the higher compute and samples seen scales, smaller models tend to saturate**, indicating a bottleneck in model number of parameters.

Data efficiency on Re-LAION and DFN. As we see from Fig. 11, MaMMUT exhibits consistently more superior scaling with respect on training data size on both Re-LAION-1.4B and DFN-1.4B. This supports the conclusion that **MaMMUT is more data efficient across multiple training datasets.**

LR Scheduler	GPU	Dataset	MWh	GPU Hours
NVIDIA A100				
cosine	NVIDIA-A100	DataComp-1.4B	2.59e+05	1.03e+06
const-cooldown	NVIDIA-A100	DataComp-1.4B	1.43e+05	5.72e+05
const	NVIDIA-A100	DataComp-1.4B	9.30e+04	3.72e+05
cosine	NVIDIA-A100	Re-LAION-1.4B	3.91e+04	1.56e+05
const-cooldown	NVIDIA-A100	Re-LAION-1.4B	1.70e+04	6.79e+04
const	NVIDIA-A100	Re-LAION-1.4B	4.61e+03	1.84e+04
		A100 subtotal:	**5.56e+05**	**2.22e+06**
NVIDIA H100				
cosine	NVIDIA-H100	DataComp-1.4B	2.09e+04	2.98e+04
cosine	NVIDIA-H100	Re-LAION-1.4B	1.06e+04	1.52e+04
		H100 subtotal:	**3.15e+04**	**4.50e+04**
		Total:	**5.87e+05**	**2.27e+06**

Table 4: Total GPU compute and energy consumption for scaling law derivation experiments.

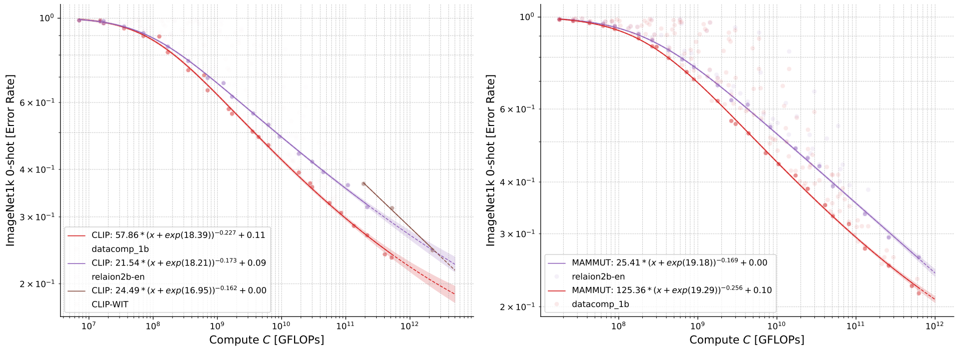

(a) CLIP on WIT, Re-LAION, DataComp

(b) MaMMUT on Re-LAION, DataComp

Figure 7: Scaling laws for IN1k 0-shot performance of openCLIP (left) and openMaMMUT (right), comparing training on DataComp-1.4B and Re-LAION-1.4B. For CLIP we have 3 additional points for OpenAI CLIP [7] models trained on WIT-400M dataset for reference.

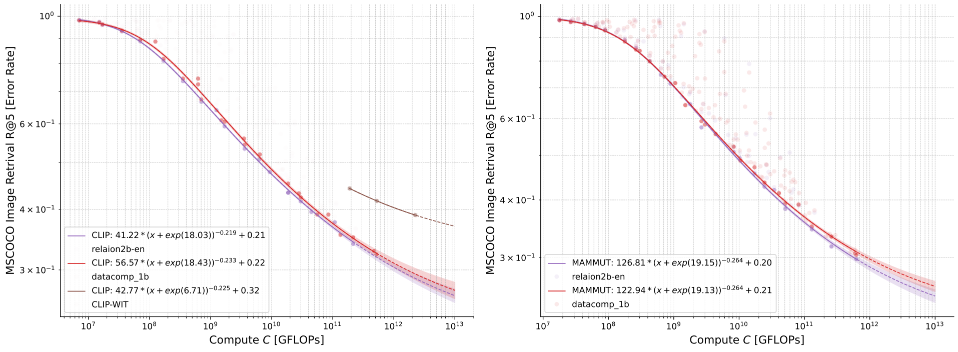

(a) CLIP on WIT, Re-LAION, DataComp

(b) MaMMUT on Re-LAION, DataComp

Figure 8: Scaling laws for MS-COCO image retrieval performance (1- Recall@5) of openCLIP (left) and openMaMMUT (right), comparing training on DataComp-1.4B and Re-LAION-1.4B. For CLIP models we have 3 additional points for OpenAI CLIP [7] trained on WIT-400M dataset for reference.

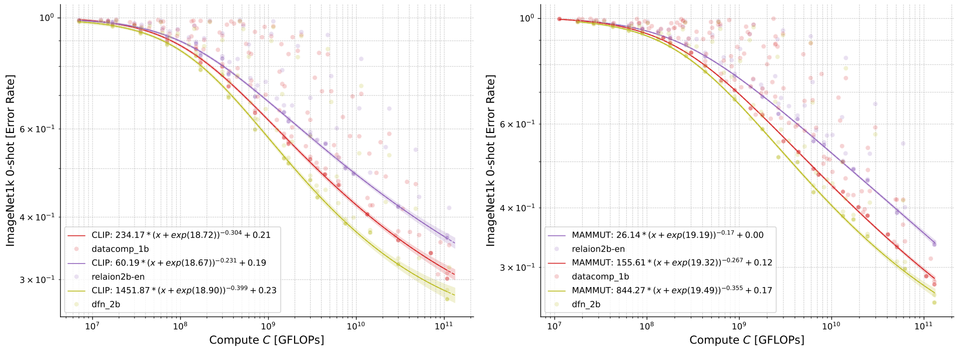

(a) CLIP on Re-LAION, DataComp, DFN

(b) MaMMUT on Re-LAION, DataComp, DFN

Figure 9: Scaling laws for IN1k 0-shot performance of openCLIP (left) and openMaMMUT (right), comparing training on Re-LAION-1.4B, DataComp-1.4B and DFN-1.4B. Training on DFN-1.4B results in superior performance across scales consistently for both architectures.

Model	ImageNet-1k				MS-COCO Retrieval			
	$\boldsymbol{A_c}$	$\boldsymbol{B_c}$	$\boldsymbol{\alpha_c}$	$\boldsymbol{E_c}$	$\boldsymbol{A_c}$	$\boldsymbol{B_c}$	$\boldsymbol{\alpha_c}$	$\boldsymbol{E_c}$
openCLIP	57.862	18.391	-0.227	0.111	53.913	18.413	-0.230	0.216
openMaMMUT	79.970	19.111	-0.233	0.076	119.751	19.122	-0.263	0.212

(a) Fitted scaling law parameters $(A_c, B_c, \alpha_c, E_c)$ for error rate on 0-shot ImageNet-1k classification and MS-COCO retrieval tasks, rounded to three decimal places for models trained on DataComp-1.4B.

C_0 GFLOPs	IN-1k Err. Rate $\lvert d\mathcal{L}(C_0)/dC\rvert$	COCO R@5 Err. Rate $\lvert d\mathcal{L}(C_0)/dC\rvert$
CLIP		
5.00e+10	9.85e-13	8.44e-13
1.00e+11	4.21e-13	3.60e-13
5.00e+11	5.86e-14	4.95e-14
Average: IN-1k: 4.882e-13, COCO: 4.177e-13		
MaMMUT		
5.00e+10	1.17e-12	9.65e-13
1.00e+11	4.92e-13	4.03e-13
5.00e+11	6.54e-14	5.28e-14
Average: IN-1k: 5.758e-13, COCO: 4.702e-13		

(b) Numerical values of derivatives of fitted functions with respect to compute, in points $5 \cdot 10^{10}$, $1 \cdot 10^{11}$, $5 \cdot 10^{11}$ GFLOPs for both ImageNet-1k error rate and COCO retrieval error rate (1-R@5). MaMMUT consistently exhibits higher values of $\lvert d\mathcal{L}(C_0)/dC\rvert$ which corresponds to higher decrease rate and stronger scalability.

Table 5: Estimated parameters for main scaling law fits for 0-shot ImageNet-1k classification and MS-COCO retrieval, used for openCLIP and openMaMMUT comparison in Fig. 1

Model	ImageNet-1k				MS-COCO Retrieval			
	$\boldsymbol{A_c}$	$\boldsymbol{B_c}$	$\boldsymbol{\alpha_c}$	$\boldsymbol{E_c}$	$\boldsymbol{A_c}$	$\boldsymbol{B_c}$	$\boldsymbol{\alpha_c}$	$\boldsymbol{E_c}$
openCLIP	14.769	16.725	-0.168	0.121	6.686	16.209	-0.123	0.089
openMaMMUT	1850.286	20.521	-0.379	0.198	634.190	20.256	-0.335	0.249

Table 6: Fitted scaling law parameters $(A_c, B_c, \alpha_c, E_c)$ for error rate on 0-shot ImageNet-1k classification and MS-COCO retrieval tasks, rounded to three decimal places for models trained on DataComp-1.4B with constant learning rate scheduler.

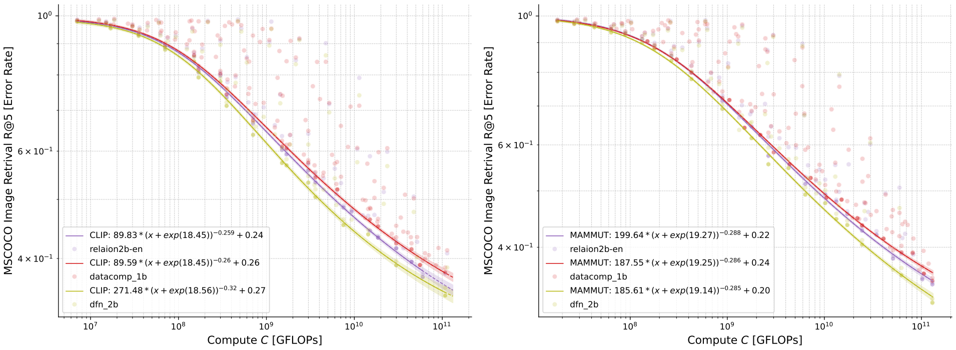

(a) CLIP on Re-LAION, DataComp, DFN

(b) MaMMUT on Re-LAION, DataComp, DFN

Figure 10: Scaling laws for MS-COCO image retrieval performance (1- Recall@5) of openCLIP (left) and openMaMMUT (right), comparing training on Re-LAION-1.4B, DataComp-1.4B and DFN-1.4B. Training on DFN-1.4B results again in superior performance across scales consistently for both architectures.

Training trial-to-trial variance. To perform trial-to-trial variance sanity check for model pre-training, ensuring that trial-to-trial variance of same runs is substantially smaller that variance due to scaling or hyperparameter tuning, we show downstream task performance on zero-shot IN1K as observed for 3 training runs of the same configuration for reference scales B-32 and B-16 on 640M samples, using same hyperparameters that correspond to minimum loss obtained in tuning, residing on Pareto front. As the results in Tab. 7 suggest, variance is negligibly small compared to difference

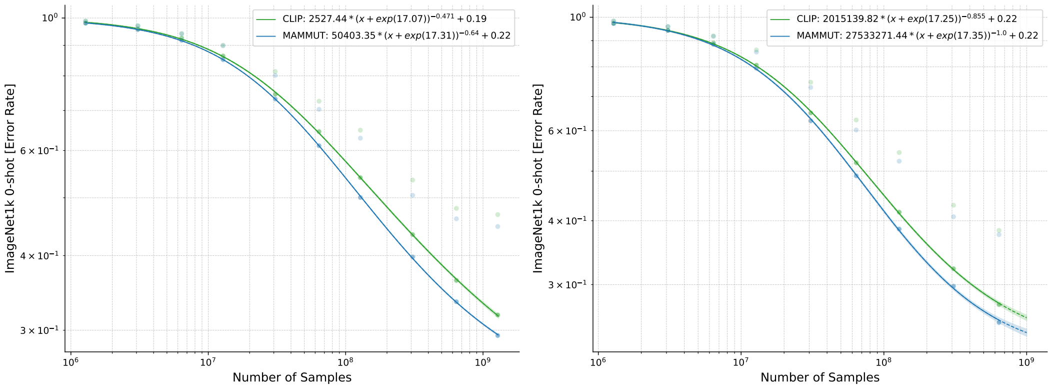

(a) CLIP vs. MaMMUT, Re-LAION-1.4B

(b) CLIP vs. MaMMUT, DFN-1.4B

Figure 11: Comparison of data efficiency for CLIP and MaMMUT via scaling laws for IN1k 0-shot classification error on Re-LAION-1.4B **(a)** and DFN-1.4B **(b)**. MaMMUT is consistently more data efficient on both datasets, which is also in accord with observations from DataComp-1.4B.

due to changing the compute scale. This allows us to conclude that measurements we use for scaling laws derivation can be distorted only insignificantly by trial-to-trial training variance, and scaling trends we observe are valid and shaped dominantly by training compute.

Trial/Training	1	2	3	$\mu \pm \sigma$
B-32 640M	0.58522	0.57866	0.58014	0.58134 ± 0.0034407
B-16 640M	0.66926	0.6668	0.6631	0.666387 ± 0.00310073
L-14 640M	0.72368	0.7203	0.72398	0.722653 ± 0.00204356

Table 7: Trial-to-trial variance control experiment. IN1k zero-shot top-1 on DataComp-1.4B, 640M samples seen. Mean μ and standard deviation σ computed for each reference scale over 3 different training runs. Hyperparameters for each reference scale training run are fixed and correspond to hyperparameters tuned to obtain minimal loss via multiple sweeps for each given reference scale. Trial to trial variance is negligible small compared to performance difference across the scales and is decreasing with increasing performance level.

B.1 Effect of the number of points used for the scaling law fits

For scaling law derivation on DataComp-1.4B (Fig. 1), we used different number of points for MaMMUT (1010 points) and CLIP (672 points). Since MaMMUT architecture was never trained before on open data like DataComp, we had to perform more rigorous hyper-parameter search than for CLIP, hence we ended up with a larger set of measurements. To understand whether the number of measurements that we have obtained affects our conclusions we conduct additional experiment to double check whether there is any difference in the obtained scaling law if working with same number of points for MaMMUT as for CLIP on DataComp-1.4B. We perform bootstrapping, sampling randomly 672 points from 1010 available points for MaMMUT, doing 10 trials, fitting scaling law for each trial and averaging the obtained scaling law coefficients. We observe that the obtained fit coefficients have no significant difference from scaling law obtained with 1000 points 8. Thus, the comparison on reduced points shows similar trends. Measurements are balanced for Re-LAION (750 vs 703 points), as well as for DFN (737 vs 732 points).

Model	$\boldsymbol{A_c}$	$\boldsymbol{B_c}$	$\boldsymbol{\alpha_c}$	$\boldsymbol{E_c}$
CLIP	57.862083	18.391321	-0.226604	0.111169
MaMMUT (full points)	125.356572	19.289384	-0.255670	0.101112
MaMMUT (same points num. as CLIP)	125.267163	19.301461	-0.255934	0.108208

Table 8: Comparison of different models with their corresponding parameters.

C Evaluating scaling law fit quality

To validate our scaling law fits, we use a threshold $C_{\text{threshold}}$ to up which we take the data for the fit. We compute RMSE for the held-out points to get a measure of how good each fit is. We compare two $C_{\text{threshold}}$ values (see Tab. 9 and Fig. 20 for DataComp-1.4B dataset). We see that both RMSE and uncertainty (the width of the confidence intervals) decreases as we take more the more pointsfor the fit.

We also compare different functional forms that can be used to fit the data: model with double saturation ($\mathcal{L}(C) = A_c \cdot (C + B_c)^{-\alpha_c} + E_c$) and without a term for irreducible error E_c:

$$\mathcal{L}(C) = A_c \cdot (C + B_c)^{-\alpha_c} \tag{3}$$

We choose first $C_{\text{threshold}} = 2.5 \cdot 10^{11}$ GFLOPs and the second $C_{\text{threshold}} = 5 \cdot 10^{11}$ GFLOPs. As we see from Tab. 9 and Tab. 10 for both values of $C_{\text{threshold}}$ double saturation form (Eq. 1) has consistently lower RMSE than the function without irreducible error. RMSE on held out points provides thus a way to select among various scaling law fits the candidate that provides better prediction accuracy for unseen scales, which in our case is the fit obtained via double saturation functional form (Eq. 1).

We see that the same trend of reducing confidence intervals and thus reducing uncertainty of the predictions when taking more points for the scaling law fit holds also for other tasks like MS-COCO image retrieval and other pre-training dataset Re-LAION-1.4B (see Fig. 20 and Fig. 13 for comparison between ImageNet-1k classification and MS-COCO retrieval and Figs. 18, 19 for Re-LAION-1.4B).

When comparing predictions with actually measured downstream task performance, we see that accuracy for the held-out points is high (Tab. 9). For instance, we measure for 3B samples seen scale on held-out points for openMaMMUT ViT L-14 zero-shot IN1K 0.784, with prediction 0.777 and 95% confidence interval (0.771, 0.783), and for openMaMMUT ViT H-14 0.795, with prediction 0.801 and 95% CI of (0.793, 0.809). Similar accuracy is observed for openCLIP, with actual measurements falling within predicted confidence intervals. **The derived scaling laws provide thus solid ground for comparison on unseen scales that have low amount of repetitions** (less than 3x in case of 3B samples seen scale when training on DataComp-1.4B or Re-LAION-1.4).

As already discussed in Sec. 3.5, the prediction for performance of MaMMUT L-14 on the larger 12.8B samples seen scale (Tab. 1, zero-shot IN1K 0.820, 95% CI (0.815, 0.826)) is therefore only made for low repetition scenario, and to validate it, dataset size larger than currently used 1.4B samples (which gives around 9x repetitions for 12.8B samples seen scale) is required. The measured 0.803 for openMaMMUT L-14 on 12.8B (Tab. 3) is thus expectedly below the prediction, as performance is diminished due to high amount of repetitions, in line with observations by previous works [41, 49].

Model	Samples Seen	GFLOPs	IN1k 0-shot acc	Predicted IN1k 0-shot acc (95% CI)	Predicted (more points) IN1k 0-shot acc (95% CI)
CLIP					
ViT-L-16	3.07e+9	4.07e+11	0.761	0.747 (0.738, 0.755)	–
ViT-L-14	3.07e+9	5.18e+11	0.766	0.753 (0.744, 0.762)	0.759 (0.751, 0.766)
ViT-H-14	3.07e+9	1.14e+12	0.784	0.773 (0.761, 0.784)	0.779 (0.770, 0.789)
RMSE: 1.26e-02	*RMSE (more points): 5.90e-03*				
MaMMUT					
mammut-ViT-L-14	1.28e+9	2.59e+11	0.749	0.743 (0.737, 0.748)	–
mammut-ViT-L-14	3.07e+9	6.22e+11	0.784	0.773 (0.765, 0.781)	0.777 (0.771, 0.783)
mammut-ViT-H-14	3.07e+9	1.43e+12	0.798	0.797 (0.787, 0.807)	0.801 (0.793, 0.809)
RMSE: 7.57e-03	*RMSE (more points): 7.57e-03*				

Table 9: Predicting held-out points on compute-optimal Pareto front based on scaling law derivation for the functional form with double saturation (Eq. 1). To check prediction accuracy when extrapolating beyond points taken for the fit, we predict starting from different compute threshold values of $C^{CLIP}_{\text{threshold}} = 4.07 \cdot 10^{11}$, $C^{MaMMUT}_{\text{threshold}} = 2.59 \cdot 10^{11}$. $C_{\text{threshold}}$ points themselves are predicted by taking smaller $C_{\text{cutoff}} = 2.5 \cdot 10^{11}$. The last column contains updated predictions made after taking additional data points up to $C_{\text{threshold}}$, showing predictions that extrapolate 2.4 and 5.5 compute factor beyond the fit for MaMMUT, and 1.3 and 2.8 for CLIP. Both confidence interval and RMSE decrease as we take more points. RMSE is consistently lower than RMSE measured for functional form without irreducible error (Tab. 10).

Model	Samples Seen	GFLOPs	IN1k 0-shot acc	Predicted IN1k 0-shot acc (95% CI)	Predicted (more points) IN1k 0-shot acc (95% CI)
CLIP					
ViT-L-16	3.07e+9	4.07e+11	0.761	0.769 (0.764, 0.773)	–
ViT-L-14	3.07e+9	5.18e+11	0.766	0.778 (0.774, 0.783)	0.777 (0.773, 0.782)
ViT-H-14	3.07e+9	1.14e+12	0.784	0.806 (0.802, 0.811)	0.805 (0.801, 0.809)
RMSE: 1.55e-02 RMSE (more points): 1.72e-02					
MaMMUT					
mammut-ViT-L-14	1.28e+9	2.59e+11	0.749	0.757 (0.754, 0.760)	–
mammut-ViT-L-14	3.07e+9	6.22e+11	0.784	0.795 (0.792, 0.798)	0.794 (0.791, 0.796)
mammut-ViT-H-14	3.07e+9	1.43e+12	0.794	0.825 (0.822, 0.828)	0.824 (0.822, 0.827)
RMSE: 1.98e-02 RMSE (more points): 2.26e-02					

Table 10: Predicting held-out points on compute-optimal Pareto front based on scaling law derivation for the functional form without irreducible error (Eq. 3). Comparing prediction quality to the functional form with double saturation (Tab. 9), using same values for C_{cutoff} and $C_{\text{threshold}}$. The last column contains updated predictions made after taking additional data points up to $C_{\text{threshold}}$. Both confidence interval and RMSE decrease as we take more points. RMSE is consistently higher than RMSE measured for functional form with double saturation that includes irreducible error (Tab. 9).

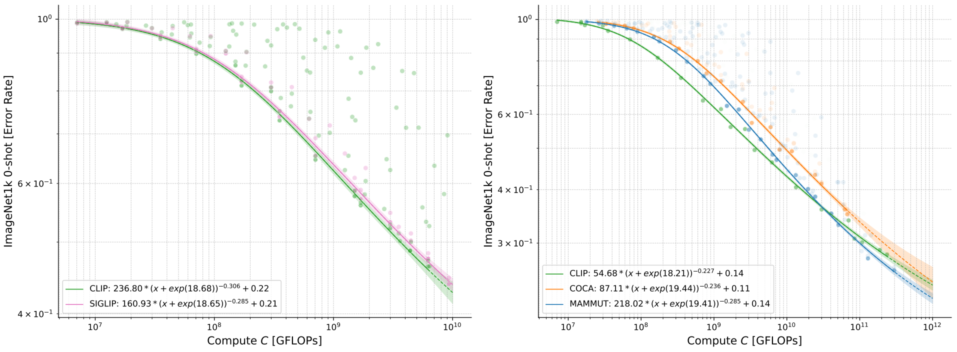

(a) CLIP vs SiGLIP on DataComp-1.4B

(b) MaMMUT vs CoCa vs CLIP on DataComp-1.4B

Figure 12: Scaling laws for ImageNet-1k 0-shot classification, comparing SigLIP (**left**) and CoCa (**right**) with standard CLIP and MaMMUT using open DataComp-1.4B dataset. SigLIP shows no benefit over standard CLIP, contrary to claims in previous work. CoCa is predicted to be less scalable than MaMMUT, while crossing CLIP is possible, although it is not clear due to high uncertainty for CoCa estimates on larger scales, as measurements on smaller scales for CoCa are not dense enough.

D Datasets comparison

Scaling laws can be also be used as a tool for dataset comparison. Here, we compare performance of models trained on two reference datasets (DataComp-1.4B and Re-LAION-1.4B) for both model architectures – CLIP and MaMMUT, for two downstream tasks – ImageNet-1k 0-shot classification and MS-COCO retrieval. For CLIP, we additionally plot OpenAI CLIP models' performance that were trained on the WIT-400M dataset. As we see from Fig. 7, **for both CLIP and MaMMUT, training on DataComp-1.4B provides superior scalability for zero-shot ImageNet-1k classification**, compared to training on Re-LAION-1.4B. At the same time, training either on Re-LAION-1.4B or DataComp-1.4B leads to similar scalability and performance on MS-COCO retrieval, with Re-LAION-1.4B being for retrieval slightly more beneficial (Fig. 8).

Using much denser measurements for scaling law derivation, we can also confirm findings from previous work [10], which showed that the closed dataset WIT-400M[7] has better scaling trend on zero-shot classification, but worse scaling trend on zero-shot retrieval when compared to LAION-2B. We observe the same for Re-LAION-1.4B, which is a safety update of LAION-2B used in [10], otherwise being same dataset with less samples due to link rot [21]. This provides further evidence for robustness of scaling law based comparison, showing consistent trends despite major difference in scaling law derivation. Previous work [10] used few samples seen scales of 3B, 12.8B and 34B, which results in high repetition given that only 2B unique samples are contained in LAION-2B [50],

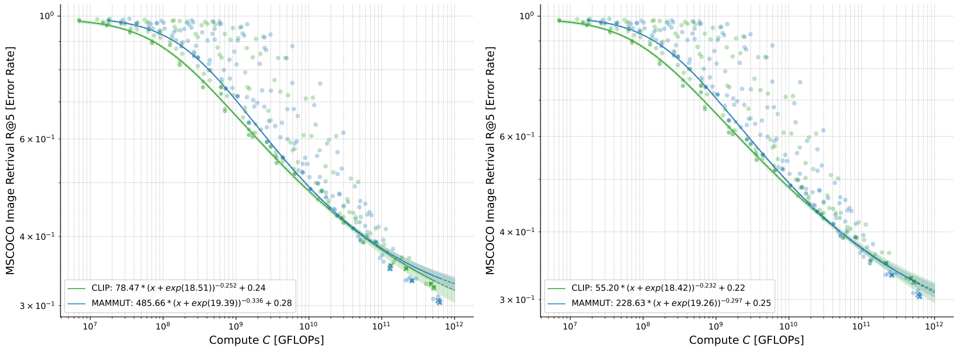

(a) Scaling law fit for MS-COCO image retrieval error rate (1-Recall@5) for DataComp-1.4B ($C_{\text{threshold}} = 2.5 \cdot 10^{11}$ GFLOPs)

(b) Scaling law fit for MS-COCO image retrievat error rate (1-Recall@5) for DataComp-1.4B using more points ($C_{\text{threshold}} = 5 \cdot 10^{11}$ GFLOPs)

Figure 13: Comparison of the fit quality for MS-COCO image retrieval error rate for openMaMMUT and openCLIP. Adding more points in (b) reduces the uncertainty of the fit, indicated by the width of bands around each curve.

while our work used denser lower samples seen scales up to 3B, doing derivation with unique samples or low repetition only. Despite these differences, derived scaling laws agree in the dataset comparison for each downstream task, predicting same scaling trends in favor of WIT-400M on classification and in favor of Re-LAION-1.4B on retrieval. DataComp-1.4B can be seen in this comparison as an improved version of Re-LAION-1.4B, with stronger scalability on classification (Fig. 7) that matches WIT-400M, while obtaining performance for retrieval (Fig. 8) that matches Re-LAION-1.4B, outperforming WIT-400M.

E Scaling behavior of other architectures

We investigate additional model architectures: SigLIP [18] (CLIP with the sigmoid loss instead of softmax), CoCa [16] and Cap [45] (pure captioner). We train these models on DataComp-1.4B in order to compare with openCLIP and openMaMMUT. Fig. 12 shows the fitted lines for these models. We see that CLIP and SigLIP have very similar scaling behavior on ImageNet-1k classification (Fig. 12 (a)) while openMaMMUT consistently overtakes CoCa on the same compute scale Fig. 12 (b). Notably, our analysis shows that **SigLIP has similar or even worse scalability than CLIP** which contradicts recent claims of SigLIP being a better choice for a vision encoder [18, 14] due to its architectural advantages. Thus, when properly controlling for same training data in our experiments, no benefits for SigLIP can be derived from the obtained scaling law trends. We also observe that text **decoder-only MaMMUT overtakes encoder-decoder CoCa on the same compute scale**, indicating that simpler and more parameter efficient architecture of MaMMUT might be preferable.

Moreover, we see (Fig. 21) that MaMMUT has superior scaling compared to Cap, showing that **combination of contrastive and captioning losses is advantageous**. We see Cap also underperforming standard CLIP, hinting that Cap as captioner only based architecture is not a good candidate for strong scalability in 0-shot regimes, making another case for contrastive losses being important part of scalable architectures for 0-shot classification. It is further important to note that Cap can use only log-likelihood based evaluation for zero-shot classification task, as opposed to CLIP and MaMMUT that in addition can use embedding similarity based evaluation thanks to their contrastive loss. As evident from Fig. 21, embedding similarity based evaluation used in openCLIP and openMaMMUT has strong advantage over log-likelihood based one. It is in addition also much cheaper in execution. Cap has thus architectural disadvantage in not being able to use similarity based evaluation due to missing contrastive loss, which leads to inferior performance in 0-shot regime.

For both comparisons, we see uncertainty getting high when extrapolating to larger scales, which makes it for instance hard to predict whether CoCa might still cross CLIP or not. To reduce uncertainty, it is thus important to both conduct dense measurements at smaller scales and not to cut off measurements at scales too small to be used for proper extrapolation.

Hyperparameter	Value
Model Architecture	mammut-ViT-L-14
Samples Seen	12.8B
Warmup Steps	6000
Global Batch Size	180,224
Learning Rate	2.5×10^{-3}
GPU Hours	3.53×10^{4}
Number of NVIDIA A100 GPUs	1024

Table 11: Training hyperparameters for openMaMMUT-L-14.

Model	Samples Seen	Warmup	Global Batch Size	Learning Rate
mammut-ViT-S-32	1.28e+06	1000	512	1.00e-03
mammut-ViT-S-32	1.28e+06	1500	512	5.00e-04
mammut-ViT-S-16	1.28e+06	1000	512	5.00e-04
mammut-ViT-S-32	3.07e+06	4000	512	5.00e-04
mammut-ViT-S-16	3.07e+06	4000	512	1.00e-03
mammut-ViT-S-32	6.40e+06	4000	1024	1.00e-03
mammut-ViT-S-32	1.28e+07	4000	2048	2.00e-03
mammut-ViT-S-16	1.28e+07	3000	2048	2.00e-03
mammut-ViT-S-32	3.07e+07	4000	4096	2.00e-03
mammut-ViT-S-16	3.07e+07	3000	4096	2.00e-03
mammut-ViT-S-32	6.40e+07	4000	4096	2.00e-03
mammut-ViT-S-16	6.40e+07	4000	4096	1.50e-03
mammut-ViT-S-32	1.28e+08	4000	8192	2.00e-03
mammut-ViT-S-14	1.28e+08	4000	8192	2.00e-03
mammut-ViT-M-16	1.28e+08	4000	8192	2.00e-03
mammut-ViT-S-14	3.07e+08	4000	16384	2.00e-03
mammut-ViT-M-16	3.07e+08	4000	16384	2.00e-03
mammut-ViT-S-14	6.40e+08	4000	16384	1.50e-03
mammut-ViT-B-16	3.07e+08	4000	16384	2.00e-03
mammut-ViT-B-32	1.28e+09	4000	16384	2.00e-03
mammut-ViT-B-16	6.40e+08	4000	32768	2.00e-03
mammut-ViT-B-14	1.28e+09	4000	90624	2.00e-03
mammut-ViT-L-16	6.40e+08	6000	45056	2.00e-03
mammut-ViT-L-14	6.40e+08	6000	45056	2.00e-03
mammut-ViT-L-14	1.28e+09	4000	90624	2.00e-03
mammut-ViT-L-16	3.07e+09	4000	91136	2.00e-03
mammut-ViT-L-14	3.07e+09	4000	91136	2.00e-03

Table 12: Hyperparameters for MaMMUT models trained on DataComp-1.4B that are located on the Pareto frontier

F Results on additional benchmarks

We also fit scaling laws on the data for other downstream tasks. In the Fig. 14 we show the scaling behavior on DataComp eval suite, which is constituted by averaging over 35 classification tasks from DataComp (see Tab.15 from [19]). Additionally, we provide scaling law fits for ImageNet-V2 and full ImageNet robustness set 0-shot classification performance for both openMaMMUT and openCLIP (Fig. 15). For all of these tasks we see the same trend - openMaMMUT is stronger scalable than openCLIP and has higher performance given the same compute at larger compute scales. This is also valid for the important robustness metrics that reflects out-of-distribution generalization (Fig. 15) - openMaMMUT shows stronger scalable robustness and outperforms openCLIP in robustness at larger compute scales.

Model	Samples Seen	Warmup	Global Batch Size	Learning Rate
ViT-S-32	1.28e+06	1500	512	5.00e-04
ViT-S-16	1.28e+06	1500	512	5.00e-04
ViT-S-16	1.28e+06	1500	512	2.00e-03
ViT-S-32	3.07e+06	1500	1024	5.00e-04
ViT-S-32	6.40e+06	4000	1024	1.00e-03
ViT-S-32	1.28e+07	4000	2048	1.00e-03
ViT-M-32	1.28e+07	3000	2048	1.00e-03
ViT-S-32	3.07e+07	4000	4096	2.00e-03
ViT-S-32	6.40e+07	4000	4096	2.00e-03
ViT-M-32	6.40e+07	10000	4096	1.00e-03
ViT-S-32	1.28e+08	6000	8192	2.00e-03
ViT-S-16	1.28e+08	6000	8192	2.00e-03
ViT-S-32	3.07e+08	8000	16384	2.00e-03
ViT-S-32	6.40e+08	4000	16384	2.00e-03
ViT-S-14	3.07e+08	4000	16384	2.00e-03
ViT-M-32	6.40e+08	6000	32800	2.00e-03
ViT-B-32	1.28e+09	15000	16384	1.00e-03
ViT-L-32	6.40e+08	4000	45056	2.00e-03
ViT-B-16-text-plus	6.40e+08	6000	32768	2.00e-03
ViT-L-32	1.28e+09	4000	90624	4.00e-03
ViT-L-16	6.40e+08	4000	45056	2.00e-03
ViT-L-32	3.07e+09	4000	91136	4.00e-03
ViT-L-14	1.28e+09	4000	90624	4.00e-03
ViT-L-16	3.07e+09	4000	91136	4.00e-03
ViT-L-14	3.07e+09	4000	91136	4.00e-03

Table 13: Hyperparameters for CLIP models trained on DataComp-1.4B that are located on the Pareto frontier.

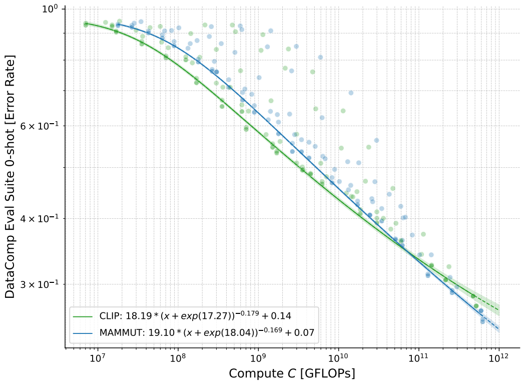

Figure 14: Scaling law on DataComp evaluation suite (average over 35 tasks, 0-shot classification), openCLIP vs. openMaMMUT comparison on DataComp-1.4B

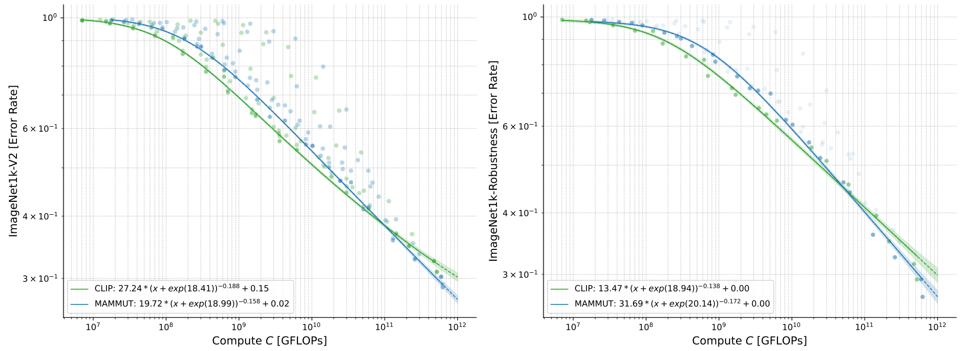

(a) CLIP vs. MaMMUT, ImageNet V2

(b) CLIP vs. MaMMUT, ImageNet Robustness

Figure 15: Scaling laws for ImageNet-v2 (left) and ImageNet robustness set (right, averaged performance across 5 datasets ImageNet-v2[27], ImageNet-R[28], ImageNet-Sketch[30], ObjectNet[31], and ImageNet-A[29]), 0-shot classification for openCLIP and openMaMMUT comparison on DataComp-1.4B

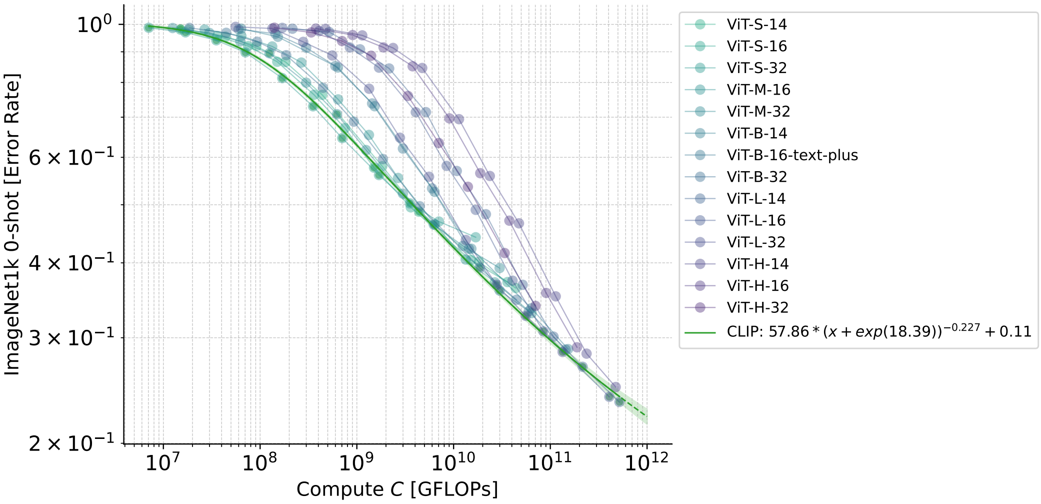

Figure 16: Detailed version of the scaling law fit for ImageNet 0-shot classification error rate for DataComp-1.4B for openCLIP. Cooler colors indicate smaller models. Bigger models are bottlenecked by samples seen scale (require larger samples seen than the smaller ones) and smaller models saturate with increased data and compute scale (over-training regime). Pareto front is composed by taking for each compute budget the points corresponding to models reaching minimal error rate for the given compute. Fit is performed through points on Pareto front.

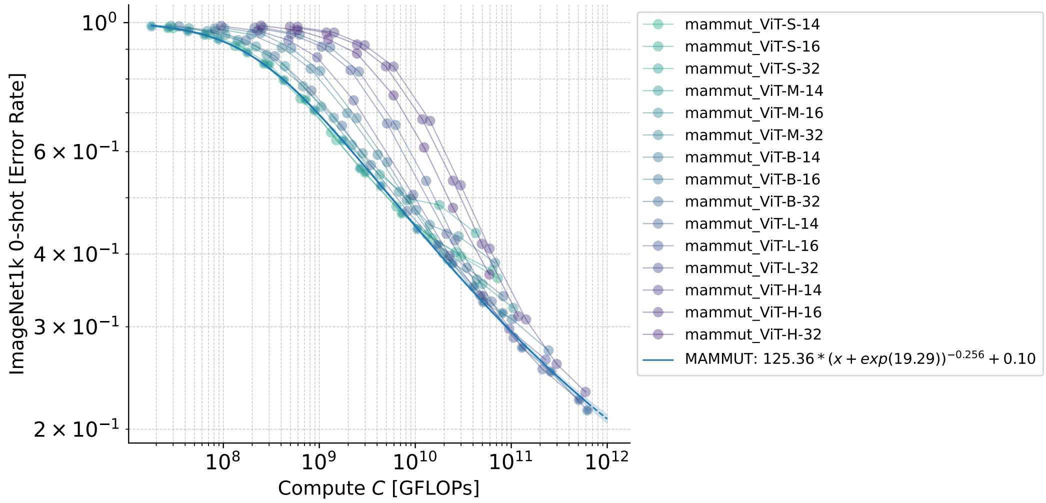

Figure 17: Detailed version of the scaling law fit for ImageNet 0-shot classification error rate for DataComp-1.4B for OpenMaMMUT. Cooler colors indicate smaller models. Bigger models are bottlenecked by samples seen scale (require larger samples seen than the smaller ones) and smaller models saturate with increased data and compute scale (overtraining regime). Pareto front is composed by taking for each compute budget the points corresponding to models reaching minimal error rate for the given compute. Fit is performed through points on Pareto front.

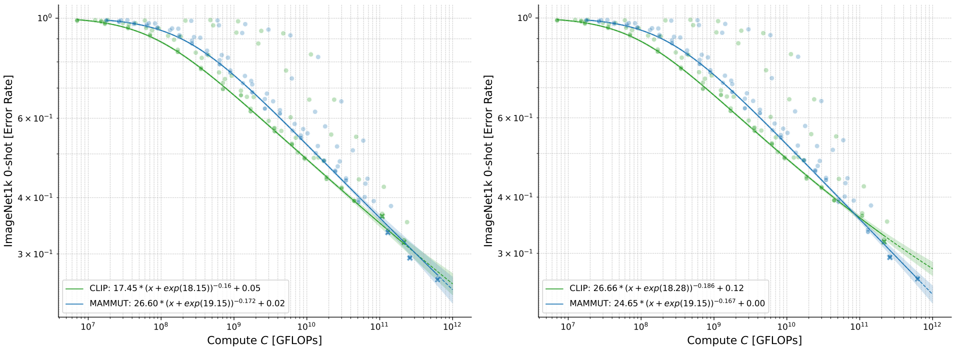

(a) Scaling law fit for
ImageNet 0-shot classification error rate
for Re-LAION-1.4B
($C_{\text{threshold}} = 2.5 \cdot 10^{11}$ GFLOPs)

(b) Scaling law fit for
ImageNet 0-shot classification error rate
for Re-LAION-1.4B using more points
($C_{\text{threshold}} = 5 \cdot 10^{11}$ GFLOPs)

Figure 18: Comparison of the fit quality for ImageNet-1k 0-shot classification error rate for openMaMMUT and openCLIP trained on Re-LAION-1.4B. Adding more points in (b) reduces the uncertainty of the fit compared to (a), indicated by the width of bands around each curve.

Name	**Width**	**Emb**	**Depth**	**Params** (M)	**GFLOPs**
ViT-S-32	384/384	384	12/12	63.09	5.51
mammut-ViT-S-32	384/384	384	12/12	85.62	13.91
ViT-S-16	384/384	384	12/12	62.26	11.75
mammut-ViT-S-16	384/384	384	12/12	84.79	20.72
ViT-S-14	384/384	384	12/12	62.21	14.3
mammut-ViT-S-14	384/384	384	12/12	84.74	23.5
ViT-M-32	512/512	512	12/12	103.12	9.74
mammut-ViT-M-32	512/512	512	12/12	134.73	22.1
ViT-M-16	512/512	512	12/12	102.02	20.84
mammut-ViT-M-16	512/512	512	12/12	133.63	34.2
ViT-M-14	512/512	512	12/12	101.95	25.37
mammut-ViT-M-14	512/512	512	12/12	133.57	39.14
ViT-B-32	768/512	512	12/12	151.28	14.54
mammut-ViT-B-32	768/512	512	12/12	183.02	26.91
ViT-B-16	768/512	512	12/12	149.62	39.51
ViT-B-16-text-plus	768/768	768	12/12	210.04	46.78
mammut-ViT-B-16	768/512	512	12/12	290.52	79.7
ViT-B-14	768/512	512	12/12	149.53	49.7
mammut-ViT-B-14	768/512	512	12/12	181.27	63.54
ViT-L-32	1024/768	768	24/12	429.95	43.59
mammut-ViT-L-32	1024/768	768	24/12	510.63	74.28
ViT-L-16	1024/768	768	24/12	427.74	132.37
mammut-ViT-L-16	1024/768	768	24/12	508.42	165.37
ViT-L-14	1024/768	768	24/12	427.62	168.61
mammut-ViT-L-14	1024/768	768	24/12	508.29	202.56
ViT-H-32	1280/1024	1024	32/24	989.02	109.81
mammut-ViT-H-32	1280/1024	1024	32/24	1191.06	192.97
ViT-H-16	1280/1024	1024	32/24	986.26	294.78
mammut-ViT-H-16	1280/1024	1024	32/24	1188.3	385.72
ViT-H-14	1280/1024	1024	32/24	986.11	370.28
mammut-ViT-H-14	1280/1024	1024	32/24	1188.14	464.39

Table 14: Hyper-parameters of architectures we consider. **Width** refers to encoder width, **Emb** refers to embedding size, **Depth** refers to number of layers, **Params** refer to the number of parameters in millions, and **GFLOPs** refer to total GFLOPs per forward pass. Entries in the form of A / B denote image and text parameters respectively. There are more parameters in MaMMUT models because of the additional cross-attention layers.

G Additional training details

In Tab. 11 we provide hyperparameters that were used for training openMaMMUT-L-14. Additionally, in the Tab. 13 and 12 we provide training hyperparameters for all models and sample seen scales that were used for scaling law fits (i.e. models that are located on the Pareto frontier) for openMaMMUT and openCLIP respectively. Tab. 14 we provide overview of model architectures parameters used for training openCLIP and openMammut.

H More details on fine-tuning for segmentation and scaling laws

Following prior work on how to benchmark vision foundation models for semantic segmentation [35], we evaluate CLIP and MaMMUT on semantic segmentation by fine-tuning them end-to-end using a linear decoder on ADE20K [34]. Regardless of the patch size used during pre-training, we interpolate the patch size of all models to 14×14, to ensure a fair comparison. We use an image input size of 224×224 and thus interpolate the positional embedding to 16×16. Hyperparameters used for training are consistent with [35], except the use of a linear learning rate warmup of 1500 steps, an epoch-based schedule of 31 epochs, and a batch size of 16 without gradient accumulation, following [36].

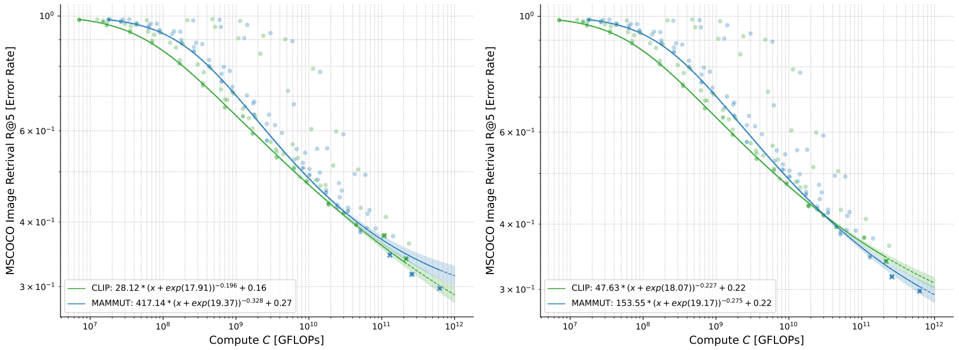

(a) Scaling law fit for MS-COCO image retrieval error rate (1-Recall@5) for Re-LAION-1.4B ($C_{\text{threshold}} = 2.5 \cdot 10^{11}$ GFLOPs)

(b) Scaling law fit for MS-COCO image retrieval error rate (1-Recall@5) for Re-LAION-1.4B ($C_{\text{threshold}} = 5 \cdot 10^{11}$ GFLOPs)

Figure 19: Comparison of the fit quality for MS-COCO image retrieval error rate for openMaMMUT and openCLIP trained on Re-LAION-1.4B. Adding more points in (b) reduces the uncertainty of the fit compared to (a), indicated by the width of bands around each curve.

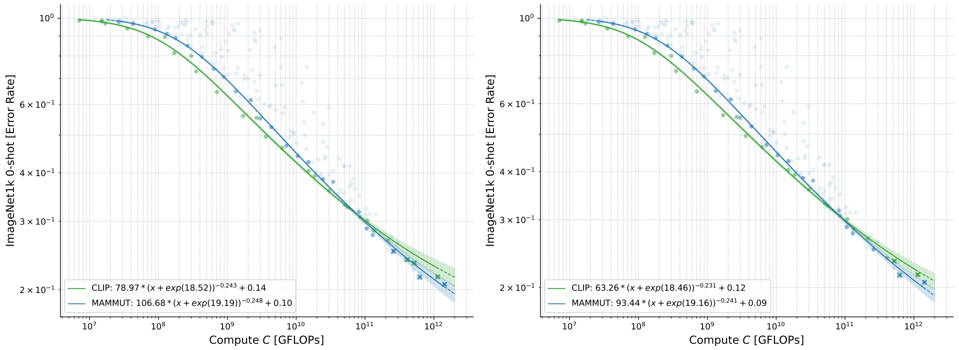

(a) Scaling law fit for ImageNet 0-shot classification error rate for DataComp-1.4B ($C_{\text{threshold}} = 2.5 \cdot 10^{11}$ GFLOPs)

(b) Scaling law fit for ImageNet 0-shot classification error rate for DataComp-1.4B using more points ($C_{\text{threshold}} = 5 \cdot 10^{11}$ GFLOPs)

Figure 20: Comparison of the fit quality for ImageNet-1k 0-shot classification error rate for openMaMMUT and openCLIP trained on DataComp-1.4B. Adding more points in (b) reduces the uncertainty of the fit compared to (a), indicated by the width of bands around each curve.

We fine-tune pre-trained models up to and including ViT-L and 3B samples seen, with different pre-training hyperparameters. We evaluate using a sliding window approach, again following [35].

Fig. 22 and Fig. 23 show the fitted scaling laws for CLIP and MaMMUT, respectively. Tab. 15 shows the corresponding estimated scaling law fit parameters.

	$\boldsymbol{A_c}$	$\boldsymbol{B_c}$	$\boldsymbol{\alpha_c}$	$\boldsymbol{E_c}$
CLIP	18.407549	17.577295	-0.209187	0.468456
MaMMUT	352.152176	18.759619	-0.356718	0.497617

Table 15: Fitted scaling law parameters $(A_c, B_c, \alpha_c, E_c)$ for segmentation error rate.

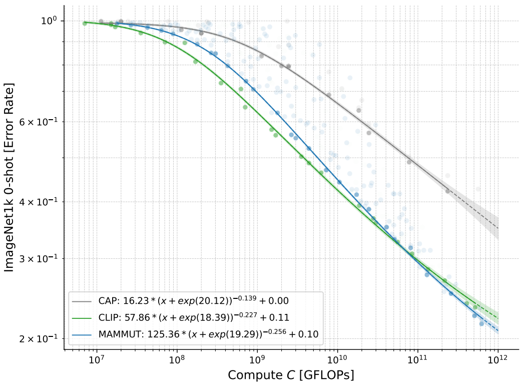

Figure 21: Scaling law fit for ImageNet-1k 0-shot classification, comparing MaMMUT, CLIP and Cap (captioning only). Cap can be only evaluated via log-likelihood, which is more expensive as similarity based evaluation used by CLIP and MaMMUT, as Cap misses contrastive loss in its architecture, which makes it disadvantageous for 0-shot setting.

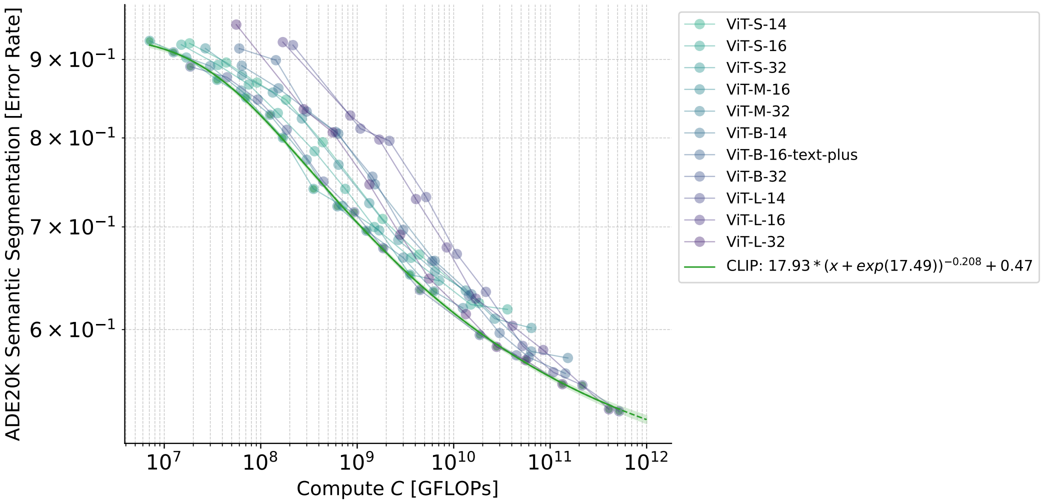

Figure 22: Downstream semantic segmentation performance of CLIP pre-trained on DataComp-1.4B and fine-tuned on ADE20K. Error rate ($1 - \text{mIoU}$).

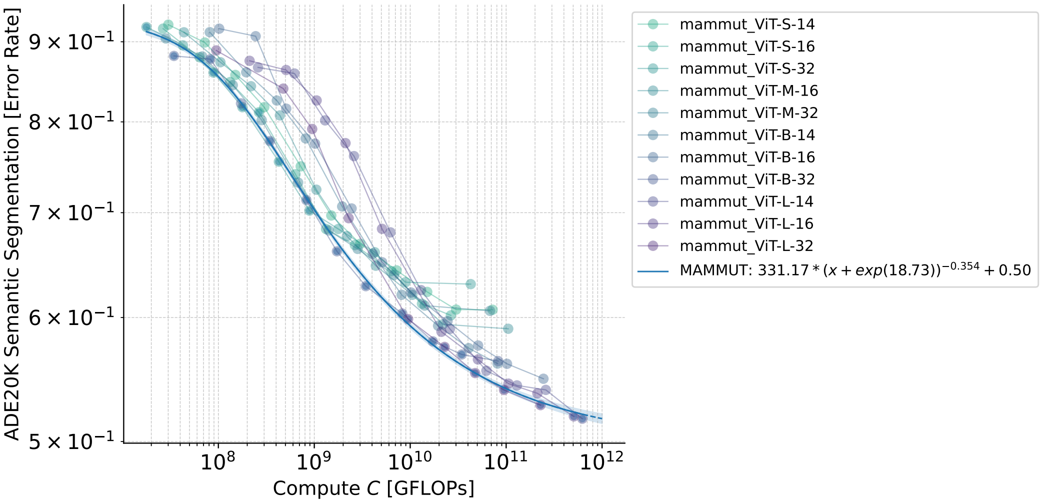

Figure 23: Downstream semantic segmentation performance of MaMMUT pre-trained on DataComp-1.4B and fine-tuned on ADE20K. Error rate $(1 - \text{mIoU})$.

I Author contributions

- **Marianna Nezhurina**: established major part of scaling law fitting procedures. Performed analysis of scaling law fit quality, derived predictions and confidence intervals. Conducted major part of data analysis. Performed initial training experiments with openCLIP and openMaMMUT. Established environments for experiments across various supercomputers. Supported compute resource acquisition. Established infrastructure for distributed dataset acquisition via Ray. Obtained Re-LAION and part of DFN dataset. Co-organized automated experiments data collection and analysis. Wrote the manuscript.
- **Tomer Porian**: co-designed and performed const lr schedule scaling law derivation experiments. Extended automated experiments execution for const lr schedule experiments. Collected and analyzed data, provided further input for scaling law fitting procedures. Co-wrote the manuscript.
- **Tommie Kerssies**: fine-tuning experiments for dense prediction segmentation, evaluating segmentation via different modes, scaling law derivation for segmentation, data collection and analysis. Co-wrote the manuscript.
- **Giovanni Puccetti**: openMaMMUT implementation in openCLIP, initial experiments with openCLIP and openMammut training. Initial co-design and implementation of automated experiments execution. Proof reading the manuscript.
- **Romain Beaumont** Re-LAION safety maintenance, hash filtering and re-packaging. Toolsets for dataset download and composition. Proof reading the manuscript.
- **Mehdi Cherti**: led the project, supported compute resource acquisition. Co-established environments for experiments across various supercomputers. Obtained DataComp, DFN and part of Re-LAION dataset. Designed and implemented automated experiments execution and evaluation. Wrote procedure for const lr schedule experiments. Conducted scaling law derivation experiments (DataComp, Re-LAION, DFN; openMammut, openCLIP, Cap). Designed and implemented evaluation. Organized automated experiments data collection and analysis. Collected and analysed the experimental data. Wrote the manuscript.
- **Jenia Jitsev**: led and coordinated the project, acquired compute resources. Organized data transfer (DataComp, Re-LAION) across the supercomputers. Co-established environments for experiments across various supercomputers. Co-designed automated experiments execution. Defined, designed and conducted scaling law derivation experiments (DataComp, Re-LAION, DFN; openMammut, openCLIP, CoCa, SigLIP). Collected and analysed the experimental data. Trained openMammut-L-14 on 12.8B of DataComp-1.4B, following the scaling law predictions. Led manuscript writing, wrote the manuscript.